Rotary orbital suspension culture of embryonic stem cell-derived neural stem/progenitor cells: impact of hydrodynamic culture on aggregate yield, morphology and cell phenotype

Tiago L. Laundos[1,2], Joana Silva[1,2], Marisa Assunção[1,2], Pedro Quelhas[1,2], Cátia Monteiro[1,2], Carla Oliveira[2,3,4], Maria J. Oliveira[1,2,4], Ana P. Pêgo[1,2,5,6] and Isabel F. Amaral[1,2,5]*

[1]Instituto de Engenharia Biomédica (INEB), Universidade do Porto, Portugal
[2]Instituto de Investigação e Inovação em Saúde (i3S), Universidade do Porto, Portugal
[3]Expression Regulation in Cancer Group, Institute of Molecular Pathology and Immunology of the University of Porto (IPATIMUP),
Portugal
[4]Departamento de Patologia e Oncologia, Faculdade de Medicina, Universidade do Porto, Portugal
[5]Faculdade de Engenharia, Universidade do Porto, Portugal
[6]Instituto de Ciências Biomédicas Abel Salazar (ICBAS), Universidade do Porto, Portugal
*Correspondence to: Isabel F. Amaral, Instituto de Engenharia Biomédica (INEB), Rua Alfredo Allen 208, 4200–135 Porto, Portugal. E-mail: iamaral@ineb.up.pt

Originally published in *J Tissue Eng Regen Med. 2017 Aug;11(8):2227-2240. doi: 10.1002/term.2121.*

INSTITUTO
DE INVESTIGAÇÃO
E INOVAÇÃO
EM SAÚDE
UNIVERSIDADE
DO PORTO

Rua Alfredo Allen, 208
4200-135 Porto
Portugal
+351 220 408 800
info@i3s.up.pt
www.i3s.up.pt

ABSTRACT

Embryonic stem (ES)-derived neural stem/progenitor cells (ES-NSPCs) constitute a promising cell source for application in cell therapies for the treatment of central nervous system disorders. In this study, a rotary orbital hydrodynamic culture system was applied to single-cell suspensions of ES-NSPCs, to obtain homogeneously-sized ES-NSPC cellular aggregates (neurospheres). Hydrodynamic culture allowed the formation of ES-NSPC neurospheres with a narrower size distribution than statically cultured neurospheres, increasing orbital speeds leading to smaller-sized neurospheres and higher neurosphere yield. Neurospheres formed under hydrodynamic conditions (72 h at 55 rpm) showed higher cell compaction and comparable percentages of viable, dead, apoptotic and proliferative cells. Further characterization of cellular aggregates provided new insights into the effect of hydrodynamic shear on ES-NSPC behaviour. Rotary neurospheres exhibited reduced protein levels of N-cadherin and β-catenin, and higher deposition of laminin (without impacting fibronectin deposition), matrix metalloproteinase-2 (MMP-2) activity and percentage of neuronal cells. In line with the increased MMP-2 activity levels found, hydrodynamically-cultured neurospheres showed higher outward migration on laminin. Moreover, when cultured in a 3D fibrin hydrogel, rotary neurospheres generated an increased percentage of neuronal cells. In conclusion, the application of a constant orbital speed to single-cell suspensions of ES-NSPCs, besides allowing the formation of homogeneously-sized neurospheres, promoted ES-NSPC differentiation and outward migration, possibly by influencing the expression of cell–cell adhesion molecules and the secretion of proteases/extracellular matrix proteins. These findings are important when establishing the culture conditions needed to obtain uniformly-sized ES-NSPC aggregates, either for use in regenerative therapies or in in vitro platforms for biomaterial development or pharmacological screening.

Keywords: neural stem cells; hydrodynamic culture; cell differentiation; cell migration; cell–cell adhesion molecules; extracellular matrix deposition; matrix metalloproteinases; 3D fibrin hydrogel

1. INTRODUCTION

Transplantation of neural stem/progenitor cells (NSPCs) has emerged as a promising therapy to overcome the limited capacity of endogenous neural progenitors to replace injury-induced lost cells and that of the central nervous system (CNS) to repair (Martino and Pluchino, 2006). Accumulating evidence shows that NSPCs transplanted into animal models of acute and chronic neurodegenerative disorders are able to contribute to cell replacement and neuroprotection, leading to improved functional recovery (Lindvall and Kokaia, 2010). For this reason, clinical trials have been approved to assess the safety and preliminary efficacy of NSPC transplantation, either of human CNS origin or derived from human embryonic stem cells (ESCs) (https://clinicaltrials.gov/). ESCs, due to their pluripotency, unlimited self-renewal and genetic flexibility, constitute an attractive donor source for NSPC-based therapies (Thompson and Bjorklund, 2015). With the establishment of reproducible protocols for efficient derivation of NSPCs from both mouse and human ESCs, large quantities of ES-NSPCs suitable for cell replacement therapies may be provided. Commitment of ESCs to the neural fate is efficiently attained in chemically defined medium and adherent monocultures (Ying *et al.*, 2003; Chambers *et al.*, 2009) or, alternatively, in suspension cultures, where ESCs are allowed to form multicellular aggregates called embryoid bodies (EBs), followed by treatment with neural induction factors (Dhara and Stice, 2008). ES-NSPCs generated by either of these culture systems can be

INSTITUTO
DE INVESTIGAÇÃO
E INOVAÇÃO
EM SAÚDE
UNIVERSIDADE
DO PORTO

Rua Alfredo Allen, 208
4200-135 Porto
Portugal
+351 220 408 800
info@i3s.up.pt
www.i3s.up.pt

purified and expanded as monolayer cultures and/or induced to form free-floating spheres. Although for transplantation purposes, both cellular aggregates (Kumagai *et al.*, 2009; Johnson *et al.*, 2010) and single-cell suspensions of ES-NSPCs (Lu *et al.*, 2012) have been used, evidence points out that NSPC transplantation in the form of cellular aggregates improves graft survival and differentiation (Johann *et al.*, 2007). In contrast to single-cell suspensions, cellular aggregates preserve both endogenous extracellular matrix (ECM) and cell–cell and cell–ECM interactions, which contribute to the establishment of a more favourable microenvironment for cell survival following transplantation.

A critical issue when considering the use of NSPCs in the form of aggregates is to obtain sufficient aggregates with homogeneous and reproducible size. Cells within cellular aggregates are exposed to concentration gradients of nutrients, oxygen, endogenous/exogenous soluble factors and metabolic by-products, existing from the outer edge of the aggregate to the core, which may compromise cell viability and proliferation and eventually lead to uncontrolled differentiation (Sargent *et al.*, 2010). Therefore, the use of homogeneously-sized aggregates contributes to reducing the heterogeneity of cell populations between aggregates, while allowing the transplantation of reproducible cell numbers. Floating aggregates of ES-NSPCs (also termed neurospheres) are typically obtained under static suspension culture, placing ES-NSPCs in serum-free medium on a non-adhesive substrate and exposing cells to mitogens (epidermal growth factor-EGF and/or basic fibroblast growth factor-bFGF) (Abranches *et al.*, 2009; Kumagai *et al.*, 2009). As the number of neurospheres resulting from the clonal progeny of single NSPCs is usually low, cell-seeding density is tuned to promote the collision and aggregation of NSPCs, to drive the formation of more neurospheres. Still, in static suspension cultures spheroid aggregation is a concern, even at low cell densities, and heterogeneously-sized aggregates are typically obtained (Ladiwala *et al.*, 2012). To promote cell assembly while preventing spheroid aggregation, culture systems developed for cell spheroid formation, such as hanging drops and microwells, may be used to obtain uniformly sized neurospheres (Mori *et al.*, 2006). However, stationary suspension cultures present several constraints that impede efficient scale-up, such as limited supply of oxygen, nutrients and growth factors to the centre of the aggregates, which, in the case of large-diameter aggregates, may lead to the development of necrotic cores. To obtain large numbers of fetal NSPC aggregates, dynamic culture systems, such as spinner flasks and bioreactors, have been successfully explored (Sen *et al.*, 2001; Baghbaderani *et al.*, 2008). The fluid motion provided by hydrodynamic culture systems, apart from allowing control over cell assembly kinetics, preventing the stochastic collision of single cells and the agglomeration of cellular aggregates, also minimizes the establishment of nutrient/oxygen concentration gradients within the medium. NSPCs cultured under dynamic culture in these systems retain the ability to generate the three major phenotypes of the mammalian central nervous system (CNS) (Baghbaderani *et al.*, 2008). However, the effect of shear rate on the process of cell differentiation and its impact on ECM deposition and remodelling has not been explored.

In 2007, McDevitt and coworkers applied a rotary orbital hydrodynamic culture system to murine pluripotent ESCs (Carpenedo *et al.*, 2007). Besides leading to higher yields of homogeneously-sized EBs, as compared to static cultures, this laboratory-scale hydrodynamic system subsequently revealed to be suitable to examine the effect of hydrodynamic conditions on EB formation, differentiation (Sargent *et al.*, 2010) and, more recently, EB intercellular adhesion kinetics (Kinney *et al.*, 2013).

In this study, a similar rotary orbital hydrodynamic culture was applied to NSPCs generated from mouse ESCs in adherent monoculture, to obtain floating aggregates of NSPCs with homogeneous

INSTITUTO
DE INVESTIGAÇÃO
E INOVAÇÃO
EM SAÚDE
UNIVERSIDADE
DO PORTO

Rua Alfredo Allen, 208
4200-135 Porto
Portugal
+351 220 408 800
info@i3s.up.pt
www.i3s.up.pt

and reproducible size (200–250 μm in diameter). For this purpose, single-cell suspensions of ES-NSPCs were cultured under static or rotary orbital conditions and the ability of the orbital speed to modulate the size and yield of neurospheres assessed. Neurospheres obtained under both culture conditions were then characterized in terms of cell packing density and key cell biological features, viz. self-renewal ability, viability, proliferation, expression of adherens junctions molecules and ECM proteins, proteolytic activity, outward migration and expression of characteristic phenotypic markers of undifferentiated and differentiated NSPCs. Finally, we assessed whether rotary orbital shaking conditions could affect neurosphere behaviour in a three-dimensional (3D) hydrogel matrix, as hydrogel vehicles can enhance the efficacy of NSPC transplantation by providing a permissive environment for cell survival, anchorage, differentiation and integration (Li *et al.*, 2012). For this study fibrin hydrogel was selected, due to the widespread clinical use of fibrin and since fibrin has been shown to provide an adequate support for ES-NSPC anchorage, proliferation, neurite extension and differentiation *in vitro* (Willerth *et al.*, 2006; Amaral *et al.*, 2011), and following transplantation into animal models of spinal cord injury (Lu *et al.*, 2012).

2 Materials and methods

2.1 Maintenance of mouse ESCs and generation of neural stem/progenitor cells (NSPCs)

A modified mouse ESC line (46C) established at the Laboratory of Professor Austin Smith (Wellcome Trust Centre for Stem Cell Research, University of Cambridge, UK), expressing green fluorescent protein (GFP) under the promoter of the neural-specific *Sox1* gene, was used. ESCs were grown in KnockOut™ ESC/iPSC medium (Gibco) supplemented with 1% v/v penicillin–streptomycin (pen–strep), 2 μm GSK-3 inhibitor IX (Calbiochem) and 1000 U/ml leukaemia inhibitory factor (Chemicon) in six-well tissue culture plates pre-adsorbed with 0.1% w/v gelatin (Sigma). Prior to initiating neural commitment, cells were cultured at a high cell seeding density (1×10^5 cells/cm^2) for 24 h. To start monolayer differentiation, the cells were dissociated with StemPro® Accutase® (Gibco), resuspended in N2B27 medium and plated onto gelatin-coated wells at 2×10^4 cells/cm^2, the medium being renewed every 2 days. N2B27 is a 1:1 mixture of Dulbecco's modified Eagle's medium (DMEM)/F12 medium without phenol red, supplemented with 1% v/v modified N2 (Ying *et al.*, 2003) and Neurobasal™ medium (supplemented with 2% v/v B27 and 1% v/v l-glutamine) supplemented with 1% v/v pen–strep (all Gibco). At day 5 of monolayer differentiation, the cells were gently dissociated and Sox1–GFP expression analysed by flow cytometry, to assess the efficiency of neural conversion. Briefly, the cell layer was rinsed twice with phosphate-buffered saline (PBS) and incubated with StemPro Accutase (2–3 min, 37°C). After pipetting up and down thrice, dissociation into a single-cell suspension was checked under an inverted optical microscope and Accutase diluted with N2B27 medium. The cells were then spun down, counted, resuspended in FACS buffer [2% v/v fetal bovine serum (FBS) in PBS] and run on a flow cytometer (FACSCalibur™ or FACS Canto II, Becton Dickinson). Cell debris and dead cells were excluded, based on gates using forward-scatter (size) and side-scatter (cell complexity) criteria, and fluorescence gates set using undifferentiated 46C ESCs as negative control. All analysis was performed using FlowJo™ software. Cells were used whenever the level of Sox1–GFP expression exceeded 75%. A representative fluorescence histogram is shown in Figure S1 (see supporting information).

The clonogenic cell line of NSCs (NS-5 cell line), generated from 46C ESCs through *Sox1* neural lineage selection (Conti *et al.*, 2005), was also used to assess the effect of hydrodynamic culture on

INSTITUTO
DE INVESTIGAÇÃO
E INOVAÇÃO
EM SAÚDE
UNIVERSIDADE
DO PORTO

Rua Alfredo Allen, 208
4200-135 Porto
Portugal
+351 220 408 800
info@i3s.up.pt
www.i3s.up.pt

neurosphere formation within a high range of orbital speeds. NS-5 cells are positive for nestin (see supporting information, Figure S2) but, with passaging, Sox1–GFP expression is lost (Conti *et al.*, 2005). NS-5 cells were expanded in six-well uncoated tissue culture plates in Euromed-N medium (EuroClone), supplemented with 1% v/v N2 supplement (Gibco), 1% v/v pen–strep and 10 ng/ml of EGF and bFGF (PeproTech).

2.2 Rotary orbital suspension culture of NS-5 cells/ES-NSPCs

NS-5 cells/ES-NSPCs were dissociated as described above, resuspended in N2B27 medium and counted. Neurospheres were formed by seeding a single-cell suspension of NS-5 cells/ES-NSPCs at 2 × 10^5 cells/ml (2 × 10^5 Sox1-GFP$^+$ cells/ml in case of ES-NSPCs) into 35 mm non-tissue culture plastic Petri dishes (EziGrip) with 1.5 ml N2B27 medium supplemented with 10 ng/ml of both EGF and bFGF. The Petri dishes were placed on rotary orbital shakers (Fisher Scientific 2309-1CE), previously calibrated, and the dynamic suspension culture immediately initiated. The cells were cultured for 3 days at various orbital speeds in the range 50–150 rpm, the orbital speed being checked twice a day. After 48 h of cell culture, the medium was renewed by collecting the floating aggregates via gravity-induced sedimentation in conical tubes and resuspending the aggregates in 1.5 ml of fresh medium. NS-5/ES-NSPCs cultured in parallel under static conditions were used as controls. For static cultures of NS-5 cells, the Petri dishes were previously coated with 1.5% w/v agarose to prevent cell/neurosphere adhesion to the dishes.

2.3 Neurosphere morphometric analysis and yield

Neurosphere size and morphology were assessed after 72 h of cell culture, by phase-contrast microscopy. For morphometric analysis, images of at least 35 neurospheres were acquired from each Petri dish, using a ×10 magnification objective. Neurosphere diameter was computed from the correspondent neurosphere cross-sectional area, given by a semi-automatic image analysis tool developed using MatLab™ (see supporting information, Figure S3). Aggregates < 35 μm in diameter (mainly single cells or doublets) were not considered. The yield of neurospheres was determined by transferring the contents of each Petri dish to the wells of a 24-well non-tissue culture polystyrene plate and acquiring images covering the total area of the wells, using a stereoscopic magnifier coupled to a digital camera. Neurosphere suspension was diluted whenever necessary and aggregate number counted using a FIJI plug-in cell counter.

2.4 Cell proliferation in neurospheres

For cell proliferation analysis, 5-bromo-2′-deoxyuridine (BrdU, Sigma) was added to the culture medium at a final concentration of 16.3 μm and the neurospheres kept in culture for an additional 18 h. The distribution of proliferative cells within the neurospheres (BrdU$^+$ cells) was detected by immunocytochemistry in cryostat sections, while the percentage of proliferative cells was determined by immunocytometry, after neurosphere dissociation.

2.5 Immunocytochemistry

Immunocytochemistry was performed in neurosphere cryostat sections from two independent assays. For cryosectioning, the neurospheres were washed twice with PBS, fixed in 3.7% w/v paraformaldehyde (PFA) solution diluted 1:1 in culture medium (30 min, 37°C) and incubated

INSTITUTO
DE INVESTIGAÇÃO
E INOVAÇÃO
EM SAÚDE
UNIVERSIDADE
DO PORTO

Rua Alfredo Allen, 208
4200-135 Porto
Portugal
+351 220 408 800
info@i3s.up.pt
www.i3s.up.pt

overnight in 30% w/v sucrose. After embedding in OCT, the neurospheres were frozen at −20°C, cryosectioned at 16 µm thickness, processed for immunocytochemistry and observed under confocal laser scanning microscopy (CLSM) (further details are provided in Supplementary materials and methods; see supporting information).

2.6 Immunocytometry

For immunocytometry analysis, a pool of three replicate Petri dish cultures was used. For dissociation of floating aggregates, neurospheres were collected by sedimentation, rinsed twice with PBS and incubated with StemPro Accutase (10 min, 37°C, flicking the bottom of the tube every 1 min). After pipetting up and down thrice, dissociation into single-cell suspension was checked under the inverted optical microscope and the cells collected by centrifugation. Dissociated cells were then resuspended in N2B27 medium for counting and processed for immunocytometry analysis (details are provided in Supplementary materials and methods; see supporting information). Unlabelled cells were used to set fluorescence gates. Cells stained with secondary antibody only, or with the correspondent isotype control, were used to eliminate non-specific background secondary antibody staining. For BrdU analysis, samples not exposed to BrdU but processed in parallel for immunodetection of BrdU were used as negative controls. Representative fluorescence histograms are shown in Figures S4 and S5 (see supporting information).

2.7 Statistical analysis

Two to four independent experiments (carried out with ES-NSPCs obtained from a different neural commitment) were performed/parameter assessed. In each flow-cytometry analysis, 10 000 events were captured inside the gate. To analyse data from a representative experiment, the unpaired *t*-test was used after previous testing of sample distribution for normality using the Kolmogorov–Smirnov test. To analyse the effect of dynamic suspension culture (55 rpm) vs static conditions within the different independent experiments, a paired-samples *t*-test was used. To analyse the effect of hydrodynamic culture on cell viability/phenotype after neurosphere culture in a 3D hydrogel matrix, data from two independent experiments were pooled and significant differences detected using unpaired *t*-test. A 95% confidence level was considered statistically significant. Calculations were performed using IBM® SPSS® Statistics v. 20. Mean values and standard deviations (SDs) are reported, unless mentioned otherwise.

A detailed description of the methodology followed for the generation of secondary neurospheres, as well as for the analysis of average cell number/neurosphere, neurosphere surface morphology, cell viability and apoptosis, protein expression levels of β-catenin, N-cadherin, laminin and fibronectin, matrix metalloproteinases (MMP) activity, outward cell migration, as well as for neurosphere culture in a 3D fibrin hydrogel matrix, is provided in Supplementary materials and methods (see supporting information).

3 Results

3.1 Effect of rotary orbital speed on neurosphere size and yield

To assess the ability of rotary orbital speed to modulate the size and yield of neurospheres, the clonogenic NS-5 cell line was initially used to overcome the variability between neural commitment

INSTITUTO
DE INVESTIGAÇÃO
E INOVAÇÃO
EM SAÚDE
UNIVERSIDADE
DO PORTO

Rua Alfredo Allen, 208
4200-135 Porto
Portugal
+351 220 408 800
info@i3s.up.pt
www.i3s.up.pt

cultures in terms of conversion efficiency. NS-5 single-cell suspensions were cultured under static or rotary orbital conditions, using a wide range of orbital speeds (60–150 rpm) and neurosphere size and morphology assessed after a 3 day culture period, using phase-contrast microscopy. As compared to static culture conditions, rotary suspension culture led to the formation of more regularly-shaped cellular aggregates with spheroid-like morphology, and to fewer single cells remaining in suspension (Figure 1A). The generated hydrodynamic forces also prevented cell/neurosphere adhesion to the bottom of Petri dishes, overcoming the need for an agarose coating. Image analysis revealed a decrease in neurosphere average diameter with increasing orbital speeds (Figure 1B). The impact of the orbital speed on neurosphere size was particularly evident at lower speeds (60–80 rpm), for which significant differences were observed between 10 rpm speed steps, and for speeds ≥ 130 rpm (p < 0.01; see supporting information, Table S1). With increasing orbital speeds, neurosphere size distribution became narrower and distribution peaks more evident, indicating tighter control of the neurosphere diameter (Figure 1C). Neurospheres were subsequently observed under a stereoscopic magnifier for yield assessment (see supporting information, Figure S6). The total number of neurospheres obtained, starting from a constant inoculation cell density, increased with increasing rotary orbital speeds, varying from ~20 (60 rpm) to > 10 000 neurospheres (150 rpm, Figure 1B). Similarly, as observed for neurosphere size, the effect of the orbital speed on neurosphere yield was more pronounced in the range 60–90 rpm, for which significant differences were observed between 10 rpm speed steps, and for speeds ≥ 130 rpm (p < 0.05; see supporting information, Table S1). Once rotary orbital suspension culture was validated as an efficient system to modulate NSC aggregate size and yield, the same was applied to ES-NSPCs, using a narrower range of orbital speeds (50–70 rpm). ES-NSPCs behaved similarly to NS-5 cells under rotary orbital suspension conditions (Figure 1D–F) and speed steps of 5 rpm were found to be sufficient to significantly influence neurosphere yield (p < 0.01; see supporting information, Table S1). Still, for the same rotary orbital speed, ES-NSPC suspension cultures led to higher neurosphere yield and smaller-sized neurospheres, as compared to NS-5 cells. Considering the envisaged neurosphere size (average diameter 200–250 μm) and the resultant neurosphere yield, 55 rpm was the rotary speed selected to culture ES-NSPCs under hydrodynamic conditions in subsequent studies.

3.2 Effect of hydrodynamic culture on neurosphere ability to generate secondary neurospheres, cell compaction, and surface morphology

The ability of NSPCs to grow as free-floating aggregates relies on their capacity to self-renewal and self-aggregate (Mori *et al.*, 2006; Ladiwala *et al.*, 2012). Therefore, to obtain insight into the effect of shear stress on ES-NSPC self-renewal, neurospheres obtained under static or hydrodynamic conditions were dissociated into single cells and their ability to form new floating aggregates evaluated. As compared to static neurospheres, rotary neurospheres led to the formation of a higher number of secondary neurospheres (p = 0.0157; Figure 2A), suggesting that hydrodynamically-cultured ES-NSPCs kept their self-renewal ability. The effect of hydrodynamic culture conditions on neurosphere cell compaction was subsequently investigated. Rotary neurospheres revealed higher packing density than static neurospheres of equivalent size, showing nuclei more densely packed and uniformly distributed throughout the cross-sectional area, and ca. two-fold higher average cell number/neurosphere (Figure 2B, C). Ultrastructural analysis further supported these findings as, on the surface of neurospheres formed under static conditions, intercellular spaces and loosely-anchored rounded cells were more easily detected (Figure 2D). It is noteworthy that a large amount

INSTITUTO
DE INVESTIGAÇÃO
E INOVAÇÃO
EM SAÚDE
UNIVERSIDADE
DO PORTO

Rua Alfredo Allen, 208
4200-135 Porto
Portugal
+351 220 408 800
info@i3s.up.pt
www.i3s.up.pt

of thin filaments with tendril-like morphology was observed on the surface of both types of neurospheres, which were attributed to cellular processes with intimate cell–ECM contact.

3.3 Effect of hydrodynamic culture on neurosphere cell viability, proliferation, and apoptosis

As hydrodynamic shear, apart from providing increased diffusion of nutrients/oxygen/soluble factors to cells in the centre of the aggregates, may also cause cell damage (Rodrigues *et al.*, 2011), we assessed the effect of rotary orbital suspension culture on ES-NSPC cell viability, proliferation and apoptosis. Cell viability analysis revealed, for static and rotary neurospheres, similar distribution and equivalent percentages of viable and non-viable cells within neurospheres (Figure 3A, B). Non-viable cells were few (<9% PI^+ cells on average) and core necrosis was not observed during the time frame of this study (see supporting information, Figure S7). After an 18 h exposure to BrdU, proliferative cells distributed evenly from the edges to the cores of the spheres were detected in both static and rotary neurospheres, and equivalent percentages of $BrdU^+$ cells were found (Figure 3C, D). Early apoptotic cells (Annexin V) and apoptotic cells with fragmented DNA (dUTP) were found uniformly distributed throughout the neurospheres, and no significant differences were found between the percentages of $TUNEL^+$ cells of static and rotary neurospheres (Figure 3E–G).

3.4 Effect of hydrodynamic culture on N-cadherin and β-catenin expression in neurospheres

Since the shear forces present in the hydrodynamic culture may affect cell assembly (Sen *et al.*, 2001; Kinney *et al.*, 2013), we assessed the impact of rotary culture on the expression of N-cadherin and *β*-catenin, two critical components of the adherens junctions. Both proteins were evenly detected at cell–cell boundaries throughout the cross-sectional area and at the edge of the neurospheres (Figure 4A–D). N-cadherin and *β*-catenin were particularly expressed at the luminal surface of neural tube-like structures (denoted by arrows) formed inside the neurospheres. The arrangement of ES-NSPCs around a lumen recapitulates that of embryonic neuroepithelial cells in the developing neural tube, in which cells with an apical–basal polarity are linked at their apical surfaces by adherens junctions (Chenn *et al.*, 1998; Copp *et al.*, 2011). As compared to static conditions, hydrodynamically-cultured neurospheres revealed enriched expression of *β*-catenin at the edges of neurospheres, but overall lower levels of *β*-catenin at the membrane of cells within the core (Figure 4D, arrowheads). Quantitative analysis by western blot of neurosphere cell lysates for rotary neurospheres revealed reduced levels of N-cadherin ($p = 0.0160$) and *β*-catenin ($p = 0.0242$; Figure 4E) in comparison to the levels of the same adherens junction proteins in static cultures. Despite the latter fact, the ratio between N-cadherin and *β*-catenin remained unchanged (data not shown).

3.5 Effect of hydrodynamic culture on laminin and fibronectin expression, proteolytic activity and migration ability of neurospheres

To evaluate the effect of shear stress imposed by the hydrodynamic conditions on ECM deposition, we assessed the expression of two ECM proteins present in the developing neuroepithelium and expressed in retinoic acid-treated EBs (Campos *et al.*, 2004; Copp *et al.*, 2011; Sart *et al.*, 2014), viz. laminin and fibronectin. Cryostat sections of ES-NSPC neurospheres demonstrated that laminin is broadly expressed within the intercellular spaces (Figure 5A, B), diffusely distributed or organized as

INSTITUTO
DE INVESTIGAÇÃO
E INOVAÇÃO
EM SAÚDE
UNIVERSIDADE
DO PORTO

Rua Alfredo Allen, 208
4200-135 Porto
Portugal
+351 220 408 800
info@i3s.up.pt
www.i3s.up.pt

aggregates with punctate or plaque-like morphology, possibly due to different stages of laminin–matrix assembly (Hamill *et al.*, 2009). Laminin expression was also detected in the luminal surface of neural tube-like structures, as found in the embryonic neural tube (Copp *et al.*, 2011). Neurospheres exposed to shear stress typically displayed a higher expression of laminin at the edges of the neurospheres (Figure 5B) and revealed two-fold higher average laminin fluorescence intensity levels (p = 0.003; Figure 5C). As compared to laminin, fibronectin expression was detected at a lower level, being found in a dotted pattern throughout the neurosphere sections or forming a fibrillar network in neural rosettes (Figure 5D, E). Fibronectin expression was particularly evident at the edges of rotary neurospheres (Figure 5E), as described for laminin. Still, in contrast to laminin, no significant differences were found between the fluorescence intensity levels found for both rotary and static neurospheres (Figure 5F). Based on the differences found for laminin expression, we examined the activity of two proteases involved in ECM remodelling during neural development, viz. MMP-2 and MMP-9 (Fujioka *et al.*, 2012), secreted into the culture medium. Rotary neurospheres consistently revealed higher levels of MMP-2 activity (p = 0.008; Figure 5G). The levels of MMP-9 activity detected were much lower and no significant differences were found among conditions. We hypothesized that the higher expression of laminin and MMP-2 activity in hydrodynamically-cultured neurospheres might translate into a different cell migration capability. To test this assumption, we examined cell outward migration from neurospheres cultured on two-dimensional (2D) substrates or 3D hydrogels permissive to NSPC migration, viz. on poly-d-lysine and laminin (PDL-LN)-coated wells (Flanagan *et al.*, 2006) or 3D fibrin hydrogels (Willerth *et al.*, 2006). When cultured on PDL-LN, rotary neurospheres exhibited 1.6-fold higher cell outgrowth area than static neurospheres (p = 0.005; Figure 5H–J), suggesting higher migratory ability. On fibrin gels, the same trend was observed, although significant differences were not found (p = 0.066; Figure 5K–M).

3.6 Effect of hydrodynamic culture on cell phenotype in neurospheres

The analysis of cell phenotype in ES-NSPC neurospheres is presented in Figure 6. Cryostat sections of neurospheres evidenced immunoreactivity to nestin (NSPC marker) in most of the cells, with nestin expression being pronounced at the edges of the neurospheres and in neural tube-like rosettes. Cells immunopositive for the early neuronal marker βIII-tubulin, and showing a concentric arrangement of neurites, were found evenly distributed within the spheroids, but βIII-tubulin filaments were more abundant in rotary neurospheres. Cells expressing GFAP (astrocytic marker) were seldom found in neurospheres from both conditions, and SSEA-1 (mouse ES marker) staining, typically localized at the cell membrane, was hardly detected. Flow cytometry analysis for rotary neurospheres consistently revealed a decrease in Nestin$^+$ cells (7.7% decrease on average; p = 0.006) and an increase in βIII-tubulin$^+$ cells (10.2% increase on average; p = 0.034), suggesting that hydrodynamic conditions induce ES-NSPC neuronal differentiation and no changes in the percentage of cells expressing GFAP or SSEA-1.

3.7 Effect of hydrodynamic culture on cell viability and cell phenotype following neurosphere culture in a fibrin hydrogel

To assess the effect of hydrodynamic culture on neurosphere behaviour in a 3D hydrogel matrix, neurospheres were embedded in fibrin hydrogels and cultured for 14 days under neuronal differentiation conditions. Hydrodynamic culture did not affect cell viability, as shown by the high percentage of viable cells found in 3D cultures of either rotary or static neurospheres at day 14 (on

INSTITUTO
DE INVESTIGAÇÃO
E INOVAÇÃO
EM SAÚDE
UNIVERSIDADE
DO PORTO

Rua Alfredo Allen, 208
4200-135 Porto
Portugal
+351 220 408 800
info@i3s.up.pt
www.i3s.up.pt

average > 94.5%; Figure 7A–C). Non-viable cells were found mostly located in the centre of the neurospheres, in both conditions. Moreover, whole-mount staining of cultures showed a similar spatial distribution of cells within the gel, revealing nestin$^+$ and βIII-tubulin$^+$ cells radially sprouting and infiltrating the gel, and the establishment of a dense neuronal network (Figure 7D–G). Still, flow cytometry analysis revealed a higher percentage of neuronal cells (βIII-tubulin$^+$ cells) in cultures of rotary neurospheres (p = 0.022), while a similar percentage of cells expressing GFAP was found (Figure 7D).

4 Discussion

In this study we explored a rotary orbital hydrodynamic culture system to induce the formation of homogeneously-sized floating aggregates of ES-NSPCs (neurospheres). By applying a range of rotary orbital speeds to single-cell suspensions of NS-5 cells/ES-NSPCs for a fixed culture period (72 h), we were able to modulate the formation of cellular aggregates, increasing orbital speeds leading to higher aggregate yield and smaller-sized neurospheres. A similar trend was reported for murine ESCs cultured under rotary orbital suspension conditions, for which higher agitation rates were found to induce the formation of a higher number of smaller-sized EBs by delaying cell assembly and spheroid formation (Sargent *et al.*, 2010). Cell-assembly kinetics of ES-derived NSCs was found to be cell-type-specific, since, for a specified orbital speed, a higher number of smaller-sized neurospheres were obtained with ES-NSPCs as compared to NS-5 cells. To assure an adequate supply of nutrients and oxygen to the core of the aggregates, we selected an orbital speed (55 rpm) leading to ES-NSPC neurospheres with diameters in the range 200–250 μm, as in mammals the maximum distance between any cell and the nearest capillary is 100–200 μm (Vander *et al.*, 1985). Cellular aggregates formed at this orbital speed displayed a more uniform spherical morphology as well as a higher cell packing density when compared to similar-sized neurospheres formed under static conditions, suggesting that neurosphere growth under these hydrodynamic culture conditions mostly resulted from cell division within the initial cell cluster, rather than from aggregation of new single cells still present in the cell suspension. Although larger than static neurospheres and with two-fold higher cell number/neurosphere (for similar-sized neurospheres), rotary neurospheres showed comparable percentages and similar distributions of viable, dead, apoptotic and proliferative cells, evidencing that hydrodynamic culture provided adequate mass transfer of oxygen and nutrients to the inner core of the spheres. Notably, ES-NSPCs derived from rotary neurospheres kept the ability to self-renew and to self-aggregate, leading to the formation of secondary neurospheres, suggesting the competence of this hydrodynamic system for serial expansion of ES-NSPCs as floating aggregates. For the same inoculation density, a higher number of secondary neurospheres was formed in hydrodynamic cultures derived from rotary neurospheres, relative to static neurospheres, despite the equivalent percentage of viable and proliferative cells. We hypothesized that the fluid shear stress imparted by the hydrodynamic culture might alter the amount and type of secreted ECM, facilitating the formation and/or cohesion of secondary neurospheres in a hydrodynamic microenvironment.

Further characterization of cellular aggregates provided new insights into the effect of hydrodynamic culture on ES-NSPC behaviour. Specifically, we observed for hydrodynamically-cultured neurospheres reduced expression of the adherens junction proteins N-cadherin and β-catenin, a two-fold increase in the levels of laminin as well as increased expression of fibronectin/laminin at the edge of the spheres, higher activity of MMP-2 and enhanced cell outward migration on laminin, and increased neuronal differentiation.

INSTITUTO
DE INVESTIGAÇÃO
E INOVAÇÃO
EM SAÚDE
UNIVERSIDADE
DO PORTO

Rua Alfredo Allen, 208
4200-135 Porto
Portugal
+351 220 408 800
info@i3s.up.pt
www.i3s.up.pt

N-cadherin is a transmembrane protein present in cell–cell adhesion junctions which contributes to NSC anchorage and quiescence in the ventricular zone neurogenic niche, by sequestering β-catenin at the cell membrane and maintaining β-catenin signalling (Zhang *et al.*, 2013). In cortical neural precursors, reduction of N-cadherin has been shown to cause decreased β-catenin-dependent transcriptional activity, premature neuronal differentiation and increased migration from the ventricular zone (Zhang *et al.*, 2013). The decrease of N-cadherin and β-catenin expression in rotary neurospheres shows that shear stress affects the establishment of cell–cell adhesion junctions in neurospheres, possibly by preventing early cell aggregation and/or leading to more relaxed cell–cell adhesion contacts. The concomitant increase in the fraction of cells staining for β-tubulin, indicating a trend for neuronal differentiation, suggests that decreased N-cadherin-mediated cell–cell adhesions may have a role in the premature differentiation of ES-NSPCs cultured under hydrodynamic shear. It is noteworthy that McDevitt and coworkers, when applying various rotary orbital speeds to ES cells, showed that E-cadherin expression and β-catenin expression/transcriptional activity in EBs were temporally modulated by the kinetics of initial cell-cell aggregation, affecting ESC cardiomyogenic differentiation (Kinney *et al.*, 2013). The higher oxygen mass transfer provided by fluid motion in hydrodynamic cultures may have also contributed to shift ES-NSPCs to differentiation, by increasing the levels of dissolved oxygen within the culture volume. In fact, hypoxia was found to be important for the maintenance of a NSC pool in neurogenic niches by keeping the levels of reactive oxygen species (ROS) low, while normoxia was shown to prime NSCs for differentiation, by upregulating glycolysis and oxidative phosphorylation and leading to increased ROS (Shyh-Chang *et al.*, 2013; Ito and Suda, 2014).

ECM deposition, assembly and remodelling provide a dynamic 3D network of proteins that contribute to intercellular cohesion and compaction of multicellular aggregates, through cell–ECM interactions. Hydrodynamic culture altered both the amount and pattern of ECM deposition, leading to higher laminin deposition, enriched expression of laminin and fibronectin at the outer peripheries of the neurospheres and higher activity of MMP-2, suggesting increased ECM remodelling. These changes can be attributed to the ES-NSPC response to fluid shear stress, in an effort to foster cell–ECM interactions and neurosphere cohesion under shear tension. In neurospheres, mechanical stimuli are possibly sensed by cadherin complexes and integrin–ECM adhesions, which, by transmitting force to the actomyosin cytoskeleton, activate a cascade of signalling events, resulting in cytoskeleton rearrangement, reinforcement of cell–ECM adhesions and activation of genes responsible for the synthesis and remodelling of ECM components (DuFort *et al.*, 2011). Our results are consistent with other studies reporting altered ECM deposition and MMP expression in cells subjected to fluid shear stress (Fridley *et al.*, 2014; Tucker *et al.*, 2014). It is noteworthy that an increase in the expression of laminin chains, but not of other ECM components (such as fibronectin), was reported for colon cancer cells cultured under fluid shear stress, as we also observed, suggesting that laminin–integrin receptors are likely involved in shear-stress mechanosensing (Avvisato *et al.*, 2007). The shear stress-induced increased laminin, apart from providing ligands for cell anchorage, possibly also contributed to sustain cell viability and proliferation of ES-NSPCs in neurospheres, due to the ability of laminin to support ES-NSPC proliferation, neuronal differentiation and neurite outgrowth (Ma *et al.*, 2008). The concomitant increase in MMP-2 activity in hydrodynamically-cultured neurospheres suggests that MMPs may be implicated in neurosphere compaction, by mediating the cleavage of ECM components and enabling cell migration and matrix remodelling. MMP-2 is able to cleave laminin and fibronectin (Nagase, 2001), as well as other ECM molecules expressed by NSPCs during CNS development. Moreover, MMP-2 has been shown to promote neural progenitor cell migration *in vitro* (Wang *et al.*, 2006) and to be involved in the neurogenic response of NSPCs after ischaemic insult in

INSTITUTO
DE INVESTIGAÇÃO
E INOVAÇÃO
EM SAÚDE
UNIVERSIDADE
DO PORTO

Rua Alfredo Allen, 208
4200-135 Porto
Portugal
+351 220 408 800
info@i3s.up.pt
www.i3s.up.pt

adult rats, possibly by modulating the niche microenvironment (Fujioka *et al.*, 2012). The higher cell outward migration observed for rotary neurospheres on PDL-LN may thus be related with the higher MMP-2 activity levels found in hydrodynamic cultures, by contributing to the proteolytic cleavage of interstitial ECM. This increase was not so evident in neurospheres cultured in fibrin hydrogels, which need to be degraded by cell-secreted proteases to allow cell invasion, a process that may involve several MMPs besides the serine protease plasmin (Man *et al.*, 2011; Brown and Barker, 2014). In an *in vivo* scenario, the higher migratory capacity of rotary neurospheres may be valuable to enhance the ability of neurosphere-derived cells to leave the immediate vicinity of the implantation site and to migrate into the host tissue.

Finally, we found that the trend for higher neuronal differentiation (higher fraction of βIII-tubulin$^+$ cells) observed in rotary neurospheres persisted following neurosphere embedding and neuronal differentiation culture for a 14 day period in a 3D fibrin hydrogel. Hydrodynamics may therefore be of interest to foster differentiation of ES-NSPC neurospheres along the neuronal lineage, prior to embedding in biomaterial-based matrices for ES-NSPC transplantation.

5 Conclusions

By applying a rotary culture to ES-NSPCs, we were able to modulate the size and yield of the ES-NSPC aggregates and to obtain homogeneously-sized neurospheres. Most importantly, our study highlights that hydrodynamic culture influences cell compaction in neurospheres, cell–cell adhesion, ECM protein expression, MMP activity, outward migration and cell phenotype after a culture period as short as 3 days. These effects should be taken into consideration when envisaging the use of hydrodynamic culture for serial passaging of ES-NSPCs, or to obtain uniformly-sized ES-NSPC aggregates for use in cell therapies or in *in vitro* platforms for pharmacological screening and biomaterial development.

INSTITUTO
DE INVESTIGAÇÃO
E INOVAÇÃO
EM SAÚDE
UNIVERSIDADE
DO PORTO

Rua Alfredo Allen, 208
4200-135 Porto
Portugal
+351 220 408 800
info@i3s.up.pt
www.i3s.up.pt

Conflict of interest

The authors declare no conflicts of interest.

Acknowledgements

The authors would like to acknowledge Professor Domingos Henrique (Instituto de Medicina Molecular, Lisbon) for providing the ES 46C cell line. This study was supported by FEDER funds through the Programa Operacional Factores de Competitividade – COMPETE (Grant No. FCOMP-01-0124-FEDER-021125) and by National Funds through FCT – Fundação para a Ciência e a Tecnologia (Grant No. PTDC/SAU-BMA/118869/2010). I. F. Amaral is supported by QREN through programme ON.2 (Grant No. NORTE-07-0124-FEDER-000005) and M. J. Oliveira is an Investigator FCT Fellow.

Author contributions

T.L.L., collection and assembly of data, data analysis and interpretation; J.S., radial outgrowth assay; M.A. and C.O., western blotting analysis and interpretation; P.Q., development of semi- and automatic image analysis tools; C.M. and M.J.O., MMP activity quantification and interpretation; A.P.P., critical review of the manuscript; and I.F.A., conception, manuscript writing and final approval of manuscript.

INSTITUTO
DE INVESTIGAÇÃO
E INOVAÇÃO
EM SAÚDE
UNIVERSIDADE
DO PORTO

Rua Alfredo Allen, 208
4200-135 Porto
Portugal
+351 220 408 800
info@i3s.up.pt
www.i3s.up.pt

REFERENCES

Abranches E, Silva M, Pradier L et al. 2009; Neural differentiation of embryonic stem cells in vitro: a road map to neurogenesis in the embryo. PLoS One 4(5): e6286.

Amaral IF, Ferreira AR, Veiga D et al. 2011;Evaluation of a fibrin gel for transplantation of embryonic stem-derived neuroprogenitors into the injured spinal cord. Histol Histopathol Cell Mol Biol 26: 291–292.

Avvisato CL, Yang X, Shah S et al. 2007; Mechanical force modulates global gene expression and β-catenin signaling in colon cancer cells. J Cell Sci 120: 2672–2682.

Baghbaderani BA, Behie LA, Sen A et al. 2008; Expansion of human neural precursor cells in large-scale bioreactors for the treatment of neurodegenerative disorders. Biotechnol Progr 24: 859–870.

Brown AC, Barker TH. 2014; Fibrin-based biomaterials: modulation of macroscopic properties through rational design at the molecular level. Acta Biomater 10: 1502–1514.

Campos LS, LeoneDP, Relvas JBet al. 2004; β1 integrins activate a MAPK signalling pathway in neural stem cells that contributes to their maintenance. Development 131: 3433–3444.

Carpenedo RL, Sargent CY, McDevitt TC. 2007; Rotary suspension culture enhances the efficiency, yield, and homogeneity of embryoid body differentiation. Stem Cells 25: 2224–2234.

Chambers SM, Fasano CA, Papapetrou EP et al. 2009; Highly efficient neural conversion of human ES and iPS cells by dual inhibition of SMADsignaling. Nat Biotechnol 27: 275–280.

Chenn A, Zhang YA, Chang BT et al. 1998; Intrinsic polarity of mammalian neuroepithelial cells. Mol Cell Neurosci

11: 183–193.

Conti L, Pollard SM, Gorba T et al. 2005; Niche-independent symmetrical selfrenewal of a mammalian tissue stem cell. PLoS Biol 3(9): e283.

Copp AJ, Carvalho R, Wallace A et al. 2011; Regional differences in the expression of laminin isoforms during mouse neural tube development. Matrix Biol 30: 301–309.

Dhara SK, Stice SL. 2008; Neural differentiation of human embryonic stem cells. J Cell Biochem 105: 633–640.

DuFort CC, Paszek MJ, Weaver VM. 2011; Balancing forces: architectural control of mechanotransduction. Nat Rev Mol Cell Biol 12: 308–319.

Flanagan LA, Rebaza LM, Derzic S et al. 2006; Regulation of human neural precursor cells by laminin and integrins. J Neurosci Res 83: 845–856.

Fridley KM, Nair R, McDevitt TC. 2014; Differential expression of extracellular matrix and growth factors by embryoid bodies in hydrodynamic and static cultures. Tissue Eng C Methods 20: 931–940.

Fujioka H, Dairyo Y, Yasunaga KI et al. 2012; Neural functions of matrix metalloproteinases: plasticity, neurogenesis, and disease. Biochem Res Int 2012, Article ID 789083, 8 pages, 2012. DOI:10.1155/2012/789083

Hamill KJ, Kligys K, Hopkinson SB et al. 2009; Laminin deposition in the extracellular matrix: a complex picture emerges. J Cell Sci 122: 4409–4417.

Ito K, Suda T. 2014; Metabolic requirements for the maintenance of self-renewing stem cells. Nat Rev Mol Cell Biol 15: 243–256.

Johann V, Schiefer J, Sass C et al. 2007; Time of transplantation and cell preparation determine neural stem cell survival in a mouse model of Huntington's disease. Exp

INSTITUTO
DE INVESTIGAÇÃO
E INOVAÇÃO
EM SAÚDE
UNIVERSIDADE
DO PORTO

Rua Alfredo Allen, 208
4200-135 Porto
Portugal
+351 220 408 800
info@i3s.up.pt
www.i3s.up.pt

Brain Res 177: 458–470. Johnson PJ, Tatara A, McCreedy DA et al. 2010; Tissue-engineered fibrin scaffolds containing neural progenitors enhance functional recovery in a subacute model of SCI. Soft Matter 6: 5127–5137.

Kinney MA, Sargent CY, McDevitt TC. 2013; Temporal modulation of β-catenin signaling by multicellular aggregation kinetics impacts embryonic stem cell cardiomyogenesis. Stem Cells Dev 22: 2665–2677.

Kumagai G, Okada Y, Yamane J et al. 2009; Roles of ES cell-derived gliogenic neural stem/progenitor cells in functional recovery after spinal cord injury. PLoS One 4(11): e7706.

Ladiwala U, Basu H, Mathur D. 2012; Assembling neurospheres: dynamics of neural progenitor/stem cell aggregation probed using an optical trap. PLoS One 7(6): e38613.

Li X, Katsanevakis E, Liu X et al. 2012; Engineering neural stem cell fates with hydrogel design for central nervous system regeneration. Progr Polym Sci 37: 1105–1129.

Lindvall O, Kokaia Z. 2010; Stem cells in human neurodegenerative disorders – time for clinical translation? J Clin Invest 120: 29–40.

Lu P, Wang Y, Graham L et al. 2012; Long-distance growth and connectivity of neural stem cells after severe spinal cord injury. Cell 150: 1264–1273.

Ma W, Tavakoli T, Derby E et al. 2008; Cell– extracellular matrix interactions regulate neural differentiation of human embryonic stem cells. BMC Dev Biol 8(90). DOI:10.1186/1471-213X-8-90.

Man AJ, Davis HE, Itoh A et al. 2011; Neurite outgrowth in fibrin gels is regulated by substrate stiffness. Tissue Eng A 17: 2931–2942.

Martino G, Pluchino S. 2006; The therapeutic potential of neural stem cells. Nat Rev Neurosci 7: 395–406.

Mori H, Ninomiya K, Kino-oka M et al. 2006; Effect of neurosphere size on the growth rate of human neural stem/progenitor cells. J Neurosci Res 84: 1682–1691.

Nagase H. 2001; Substrate specificity of MMPs. In Matrix Metalloproteinase Inhibitors in Cancer Therapy, Nj C, K A (eds). edsSpringer: Berlin, Heidelburg: 39–66.

Rodrigues CAV, Fernandes TG, Diogo MM et al. 2011; Stem cell cultivation in bioreactors. Biotechnol Adv 29: 815–829.

Sargent CY, Berguig GY, Kinney MA et al. 2010; Hydrodynamic modulation of embryonic stem cell differentiation by rotary orbital suspension culture. Biotechnol Bioeng 105: 611–626.

Sart S, Ma T, Li Y. 2014; Extracellular matrices decellularized from embryonic stem cells maintained their structure and signaling specificity. Tissue Eng A 20: 54–66.

Sen A, Kallos MS, Behie LA. 2001; Effects of hydrodynamics on cultures of mammalian neural stem cell aggregates in suspension bioreactors. Indust Eng Chem Res 40: 5350–5357.

Shyh-Chang N, Daley GQ, Cantley LC et al. 2013; Stem cell metabolism in tissue development and aging. Development 140: 2535–2547.

Thompson LH, Bjorklund A. 2015; Reconstruction of brain circuitry by neural transplants generated from pluripotent stem cells. Neurobiol Dis 79: 28–40.

Tucker RP, Henningsson P, Franklin SL et al. 2014; See-saw rocking: an in vitro model for mechanotransduction research. J Roy Soc Interface 11: e0330. DOI:10.1098/rsif.2014.0330

Vander AJ, Sherman JH, Luciano DS. 1985; Human Physiology: The Mechanisms of Body Function. McGraw-Hill: New York.

Wang L, Zhang ZG, Zhang RL et al. 2006; Matrix metalloproteinase 2 (MMP2) and MMP9 secreted by erythropoietinactivated endothelial cells promote neural progenitor cell migration. J Neurosci 26: 5996–6003.

INSTITUTO
DE INVESTIGAÇÃO
E INOVAÇÃO
EM SAÚDE
UNIVERSIDADE
DO PORTO

Rua Alfredo Allen, 208
4200-135 Porto
Portugal
+351 220 408 800
info@i3s.up.pt
www.i3s.up.pt

Willerth SM, Arendas KJ, Gottlieb DI et al. 2006; Optimization of fibrin scaffolds for differentiation of murine embryonic stem cells into neural lineage cells. Biomaterials 27: 5990–6003.

Ying QL, Stavridis M, Griffiths D et al. 2003; Conversion of embryonic stem cells into neuroectodermal precursors in adherent monoculture. Nat Biotechnol 21: 183–186.

Zhang J, Shemezis JR, McQuinn ER et al. 2013; AKT activation by N-cadherin regulates β-catenin signaling and neuronal differentiation during cortical development. Neural Dev 8(7). DOI:10.1186/ 1749-8104-8-7.

INSTITUTO
DE INVESTIGAÇÃO
E INOVAÇÃO
EM SAÚDE
UNIVERSIDADE
DO PORTO

Rua Alfredo Allen, 208
4200-135 Porto
Portugal
+351 220 408 800
info@i3s.up.pt
www.i3s.up.pt

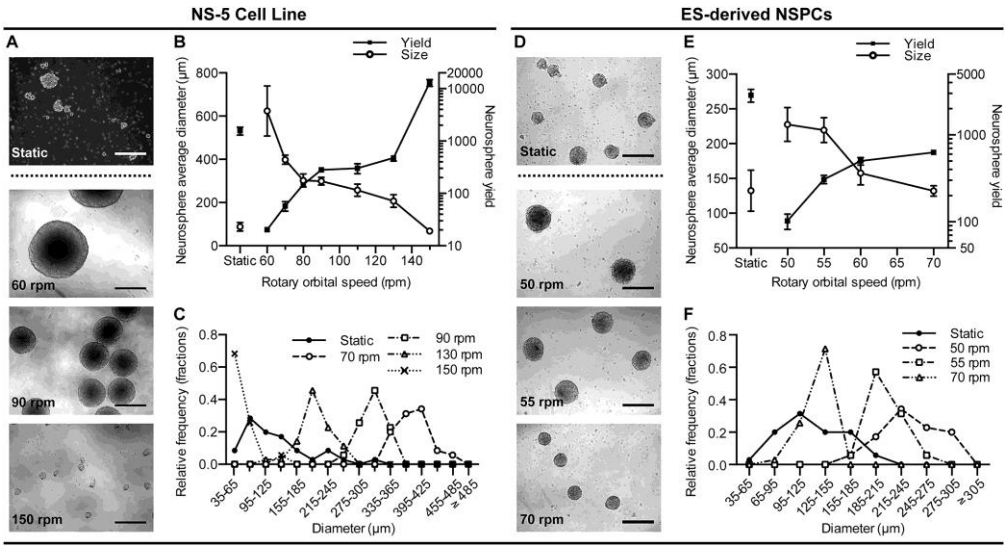

Figure 1. Effect of rotary orbital speed on neurosphere size and yield after 72 h of cell culture. The hydrodynamic culture system was applied initially to the NS-5 cell line, using orbital speeds in the range 60–150 rpm, and then to ES-derived NSPCs, using a narrower range of orbital speeds (50–70 rpm). (A, D) Phase-contrast microscopy images of floating aggregates evidencing, for both cell types, a decrease in neurosphere size with increasing rotary speed; scale bar = 300 µm. (B, E) Neurosphere average diameter and neurosphere yield (neurosphere total number/Petri dish), at variable orbital speeds; results from three Petri dish cultures are shown; see supporting information (Table S1) for individual significant differences between rotary orbital speeds and their effect of neurosphere size and yield. (C, F) Neurosphere diameter distribution at variable orbital speeds showing, for both cell types, a narrower neurosphere size distribution with increasing orbital speeds; the results shown correspond to three Petri dish cultures

INSTITUTO
DE INVESTIGAÇÃO
E INOVAÇÃO
EM SAÚDE
UNIVERSIDADE
DO PORTO

Rua Alfredo Allen, 208
4200-135 Porto
Portugal
+351 220 408 800
info@i3s.up.pt
www.i3s.up.pt

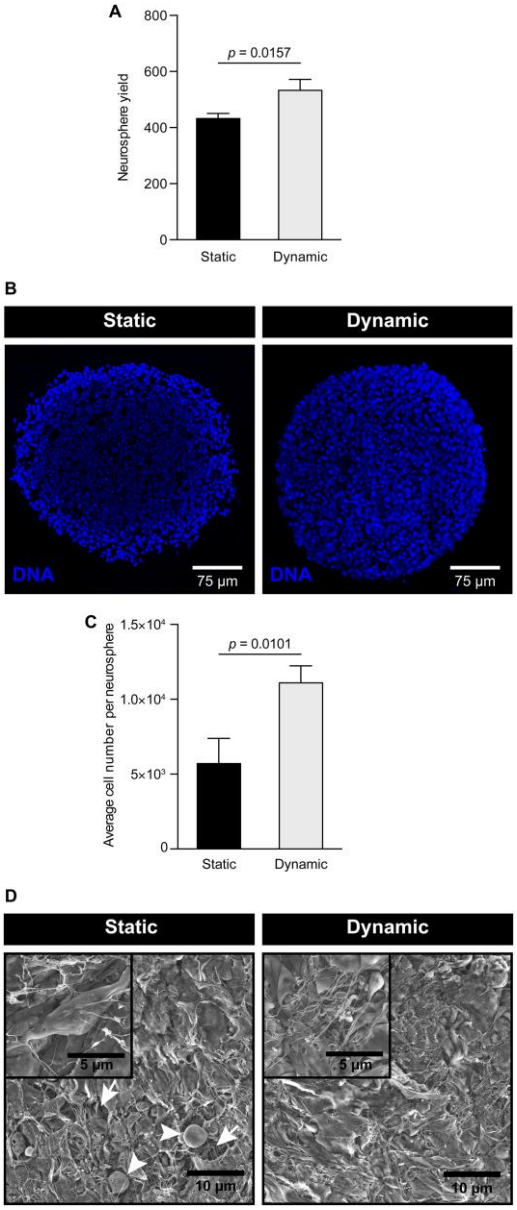

Figure 2. Self-renewal ability, cell compaction, cell number/neurosphere and surface morphology of ES-NSPC neurospheres formed under hydrodynamic (55 rpm) or static conditions. (A) Dynamic culture does not hamper the ability of neurosphere-derived cells to form secondary neurospheres: for the same inoculation density, a higher number of aggregates was formed in hydrodynamic cultures established from rotary neurospheres; results from three Petri dish cultures from a representative experiment are shown. (B) CLSM imaging of neurosphere cryostat sections previously processed for DNA staining revealing, for floating aggregates obtained under dynamic conditions, nuclei more uniformly distributed and more closely packed. (C) Average cell number/neurosphere showing, for rotary neurospheres, approximately two-fold higher cell numbers; the results shown correspond to three Petri dish cultures from a representative experiment. (D) Neurosphere surface morphology examined by SEM; intercellular spaces (arrows) and loosely-anchored rounded cells (arrowheads) are more easily detected in neurospheres obtained under static conditions. [Colour figure can be viewed at wileyonlinelibrary.com]

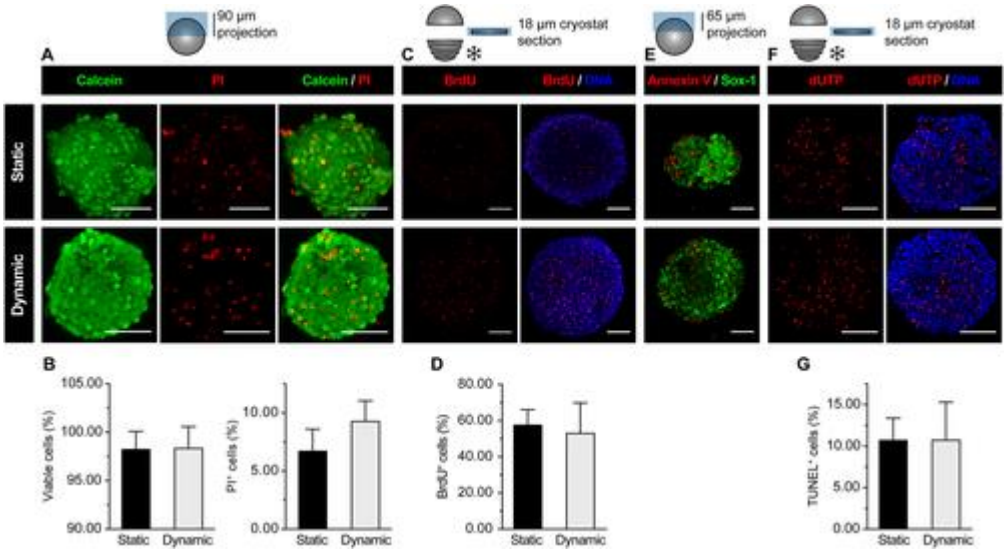

Figure 3. (A, B) Cell viability, (C, D) proliferation and (E–G) apoptosis in ES-NSC neurospheres formed under hydrodynamic (55 rpm) or static conditions. (A, C, E, F) CLSM images showing the distribution of: (A) viable (in green) and dead cells (in red); (C) proliferative cells (S-phase nuclei; BrdU); (E) early apoptotic cells (Annexin V); and (F) apoptotic cells with fragmented DNA (TUNEL). (B, D) Quantitative analysis of viable/dead cells and proliferative cells, as determined by flow cytometry in dissociated neurospheres; the results shown correspond to three independent experiments. (G) Quantitative analysis of apoptotic cells, as determined by image analysis of neurosphere cryostat sections processed for TUNEL; for each condition, five to eight cryosections from different representative neurospheres were examined; scale bar = 75 µm. [Colour figure can be viewed at wileyonlinelibrary.com]

INSTITUTO DE INVESTIGAÇÃO E INOVAÇÃO EM SAÚDE
UNIVERSIDADE DO PORTO

Rua Alfredo Allen, 208
4200-135 Porto
Portugal
+351 220 408 800
info@i3s.up.pt
www.i3s.up.pt

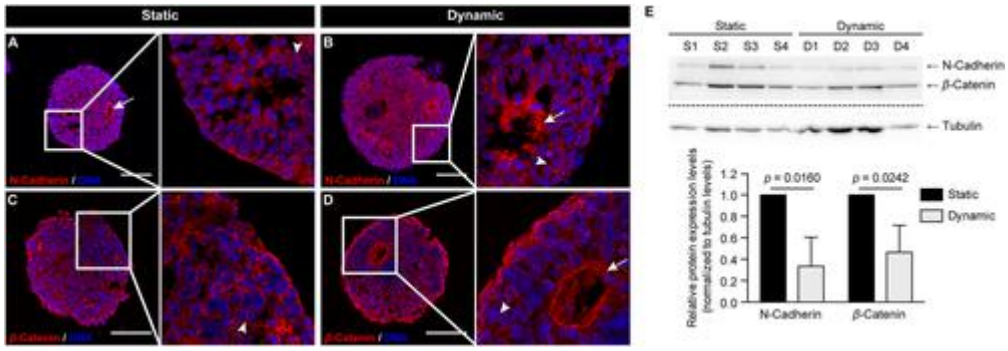

Figure 4. N-cadherin and β-catenin distribution and protein expression levels in ES-NSPC neurospheres formed under hydrodynamic (55 rpm) or static conditions. In cryostat sections of neurospheres, (A, B) N-cadherin and (C, D) β-catenin expression is evident at cell–cell boundaries (arrowheads) and particularly pronounced in the luminal surface of rosettes (arrows). Rotary neurospheres show enriched expression of β-catenin at the edge of neurospheres (D), but the overall levels of β-catenin in the core of neurospheres are lower than those of static neurospheres. (E) Western blot analysis in cell lysates from four independent experiments, revealing reduced levels of β-catenin and N-cadherin in neurospheres cultured under dynamic conditions; western blots are shown in the upper panel; scale bar = 75 μm. [Colour figure can be viewed at wileyonlinelibrary.com]

INSTITUTO
DE INVESTIGAÇÃO
E INOVAÇÃO
EM SAÚDE
UNIVERSIDADE
DO PORTO

Rua Alfredo Allen, 208
4200-135 Porto
Portugal
+351 220 408 800
info@i3s.up.pt
www.i3s.up.pt

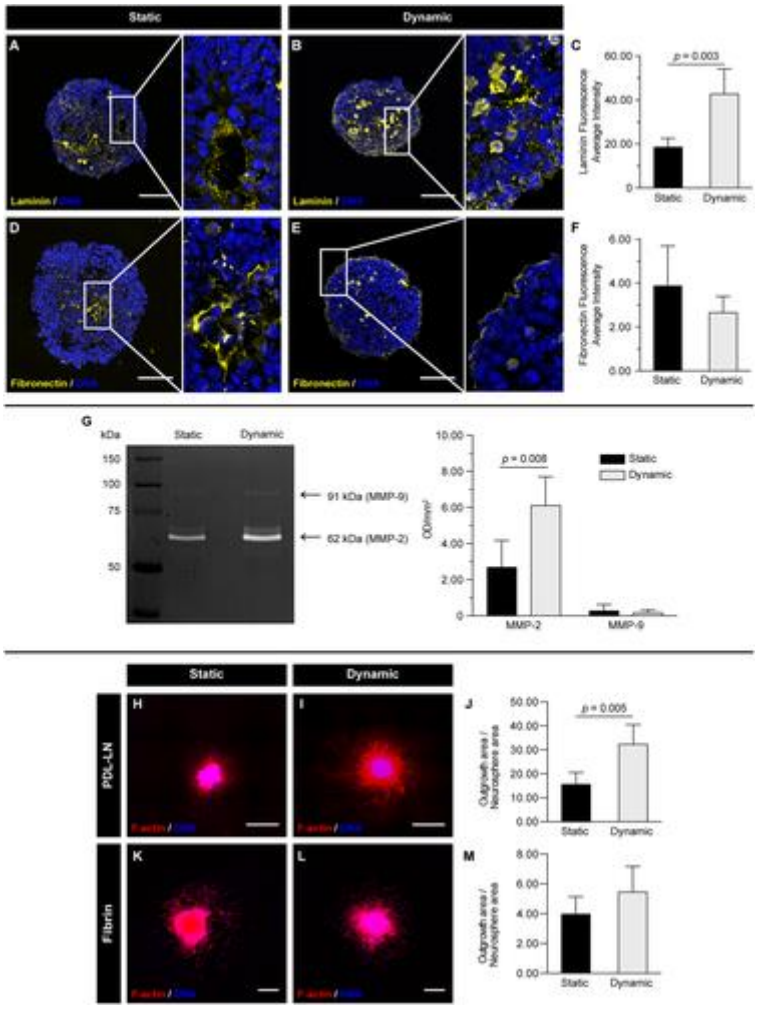

Figure 5. Characterization of ES-NSPC neurospheres formed under hydrodynamic (55 rpm) or static conditions in terms of expression of (A–C) ECM laminin and (D–F) fibronectin, (G) proteolytic activity and (H–M) migration ability. Cryostat sections of ES-NSPC neurospheres show laminin (here pseudocoloured in yellow) in neurospheres from both conditions expressed within the intercellular spaces and in neural rosettes (A, B). Fibronectin is also detected (D, E), but at a lower level, being particularly evident at the edge of the hydrodynamically-cultured neurospheres. (C, F) Quantitative image analysis of (C) laminin and (F) fibronectin expression, revealing two-fold higher laminin fluorescence intensity levels in rotary neurospheres; for each condition, six to nine cryosections from different representative neurospheres were analysed. (G) Gelatinolytic activity of MMPs secreted into the culture medium, revealing higher levels of MMP-2 activity in hydrodynamically-cultured neurospheres; results from five Petri dish cultures from a representative experiment are presented. (H–J) Cell outgrowth on PDL-LN-coated wells showing, for rotary neurospheres, 1.6-fold higher cell outgrowth area; for each condition, four wells were analysed and five randomly selected neurospheres/well examined. (K–M) Cell outgrowth on fibrin gels, showing a similar trend ($p = 0.066$), although statistically significant differences were not found; for each condition, six to nine neurospheres were analysed; scale bar = (A, B, D, E) 75 μm; (H, I, K, L) 200 μm. [Colour figure can be viewed at wileyonlinelibrary.com]

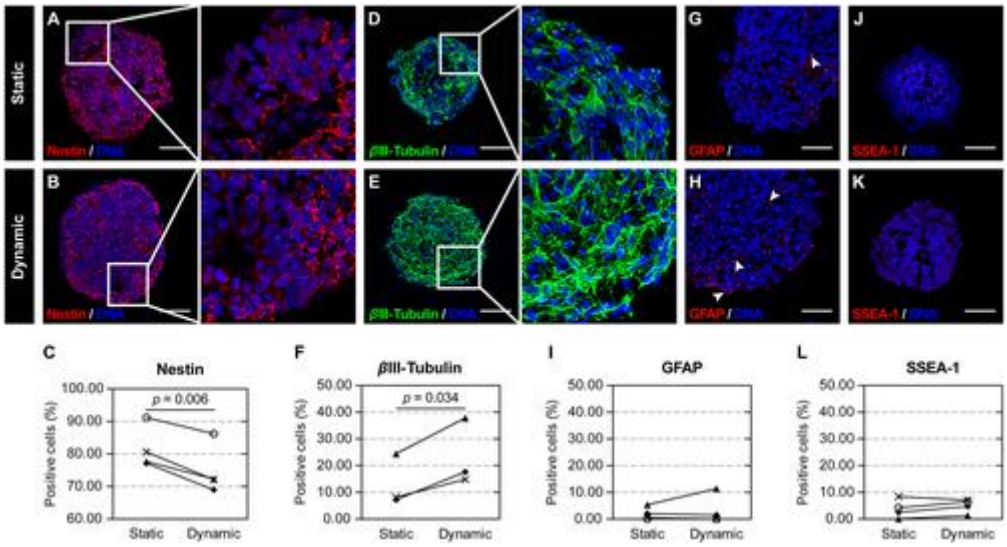

Figure 6. Phenotypic analysis of ES-NSPC neurospheres formed under hydrodynamic (55 rpm) or static conditions. CLSM images of neurosphere cryostat sections evidence immunoreactivity to nestin in most of the cells (A, B), with nestin expression being more pronounced at the edge of the neurospheres and within neural rosettes. Cells immunopositive for βIII-tubulin and with a clear neuronal morphology are found evenly distributed within the spheres (D, E), with a higher amount of βIII-tubulin filaments being observed for dynamic conditions (E). A few cells expressing GFAP were also detected in neurospheres from both conditions (G, H; arrowheads). SSEA-1 staining was hardly detected (J, K). (C, F, I, L) Flow-cytometry analysis in dissociated neurospheres revealed that dynamic conditions promote ES-NSPC differentiation, leading to a decrease in Nestin expression and to an increase in βIII-tubulin$^+$ cells; results from four independent experiments are shown; markers denote results obtained within the same independent experiment; scale bar = 75 μm. [Colour figure can be viewed at wileyonlinelibrary.com]

INSTITUTO
DE INVESTIGAÇÃO
E INOVAÇÃO
EM SAÚDE
UNIVERSIDADE
DO PORTO

Rua Alfredo Allen, 208
4200-135 Porto
Portugal
+351 220 408 800
info@i3s.up.pt
www.i3s.up.pt

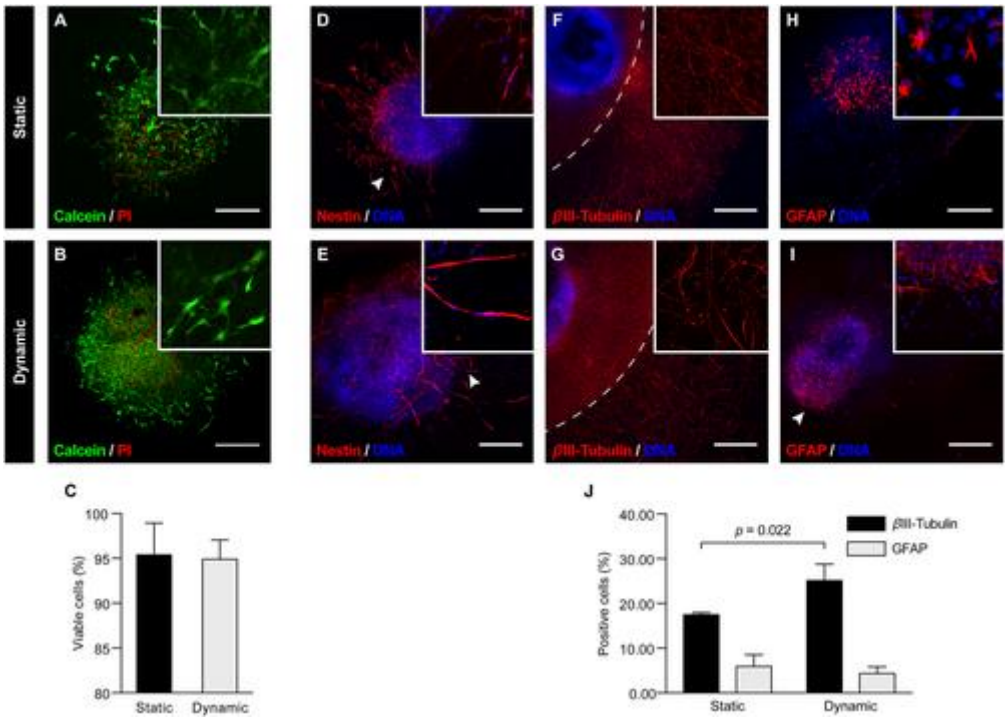

Figure 7. Cell viability and phenotypic analysis of ES-NSPC neurospheres in fibrin. Neurospheres formed under hydrodynamic (55 rpm) or static conditions were embedded in fibrin hydrogels and cultured for 14 days under neuronal differentiation conditions. (A, B) CLSM images revealed in both conditions abundant sprouting of viable cells (in green) from the neurospheres into fibrin; non-viable cells (in red) were found mostly located in the centre of the neurospheres. (C) Following dissociation and incubation with Trypan blue, similar number of viable cells were found for both conditions. 2D projections of CLSM stack images of samples processed for immunofluorescence staining revealed for both conditions cells expressing (D, E) nestin and (F, G) βIII-tubulin radially sprouting from the neurospheres and colonizing the gel, as well as (H, I) cells expressing GFAP, although to a lesser extent. (J) Flow cytometry analysis in dissociated cultures; results presented correspond to four Petri dish cultures (each containing six fibrin drops) from two independent experiments; scale bar = 300 μm. [Colour figure can be viewed at wileyonlinelibrary.com]

INSTITUTO
DE INVESTIGAÇÃO
E INOVAÇÃO
EM SAÚDE
UNIVERSIDADE
DO PORTO

Rua Alfredo Allen, 208
4200-135 Porto
Portugal
+351 220 408 800
info@i3s.up.pt
www.i3s.up.pt

Supporting Information

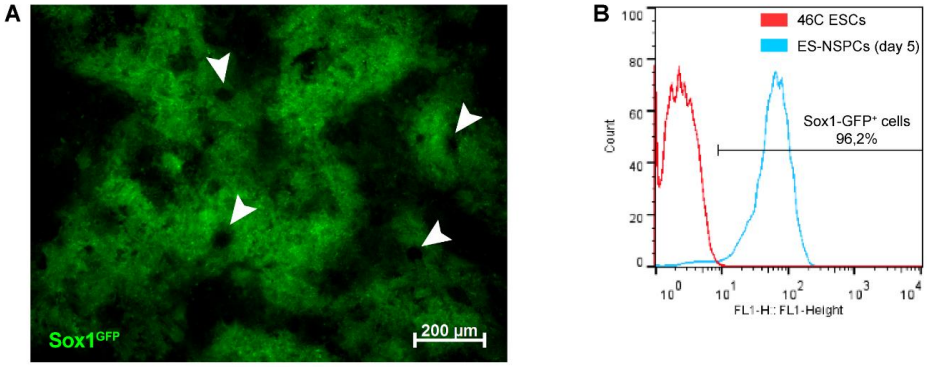

Figure S1 – Expression of Sox1^{GFP} (neuroprogenitor marker) in ES-derived NSPCs. A) Representative fluorescence microscopy image obtained at day 5 of monolayer neural commitment, showing the presence of neural progenitors (Sox1-GFP^{+} cells) organized in clusters to form neural tube-like rosettes (arrowhead). B) Flow cytometry quantitative analysis of Sox1^{GFP} expression. Undifferentiated 46C ES cells (in red) were used as the negative control, to set fluorescence gates.

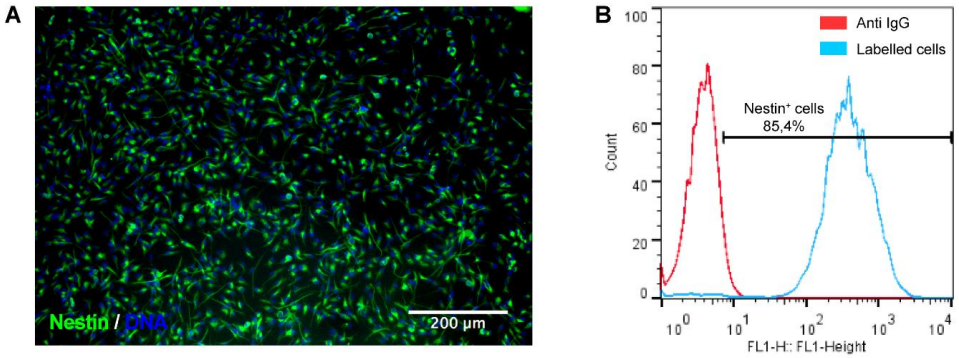

Figure S2 – Expression of Nestin (neural stem cell marker) in NS-5 cells cultured under expansion conditions. A) Fluorescence microscopy image obtained after sample processing for immunofluorescence labelling of Nestin. NS-5 cells present bipolar morphology typical of neural stem cells and a uniform expression of Nestin. B) Flow cytometry quantitative analysis of Nestin expression in NS-5 cells from the highest passage used. Cells incubated only with secondary antibody were used to quantify the contribution of non-specific adsorption of the secondary antibody to fluorescence intensity levels.

INSTITUTO
DE INVESTIGAÇÃO
E INOVAÇÃO
EM SAÚDE
UNIVERSIDADE
DO PORTO

Rua Alfredo Allen, 208
4200-135 Porto
Portugal
+351 220 408 800
info@i3s.up.pt
www.i3s.up.pt

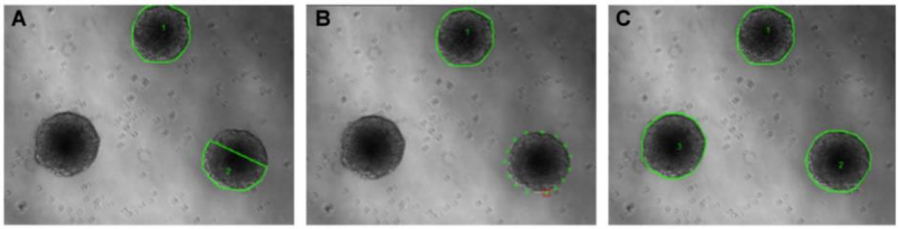

Figure S3 – Semi-automatic image analysis tool developed to determine the cross-sectional areas of neurospheres in phase-contrast images. The neurospheres borders (in green) were automatically detected (A, neurosphere 1). Whenever the edges of the spheres were not detected or inaccurately detected, the software allowed for manual delimitation/correction of the neurospheres borders (B and C). Cross-sectional areas were computed and exported for calculation of neurosphere diameter using the following equation. Scale bar: 300 µm.

$$D = 2 \cdot R \quad A = \pi \cdot R^2 \quad \leftrightarrow \quad D = \sqrt{\frac{4A}{\pi}}$$

INSTITUTO
DE INVESTIGAÇÃO
E INOVAÇÃO
EM SAÚDE
UNIVERSIDADE
DO PORTO

Rua Alfredo Allen, 208
4200-135 Porto
Portugal
+351 220 408 800
info@i3s.up.pt
www.i3s.up.pt

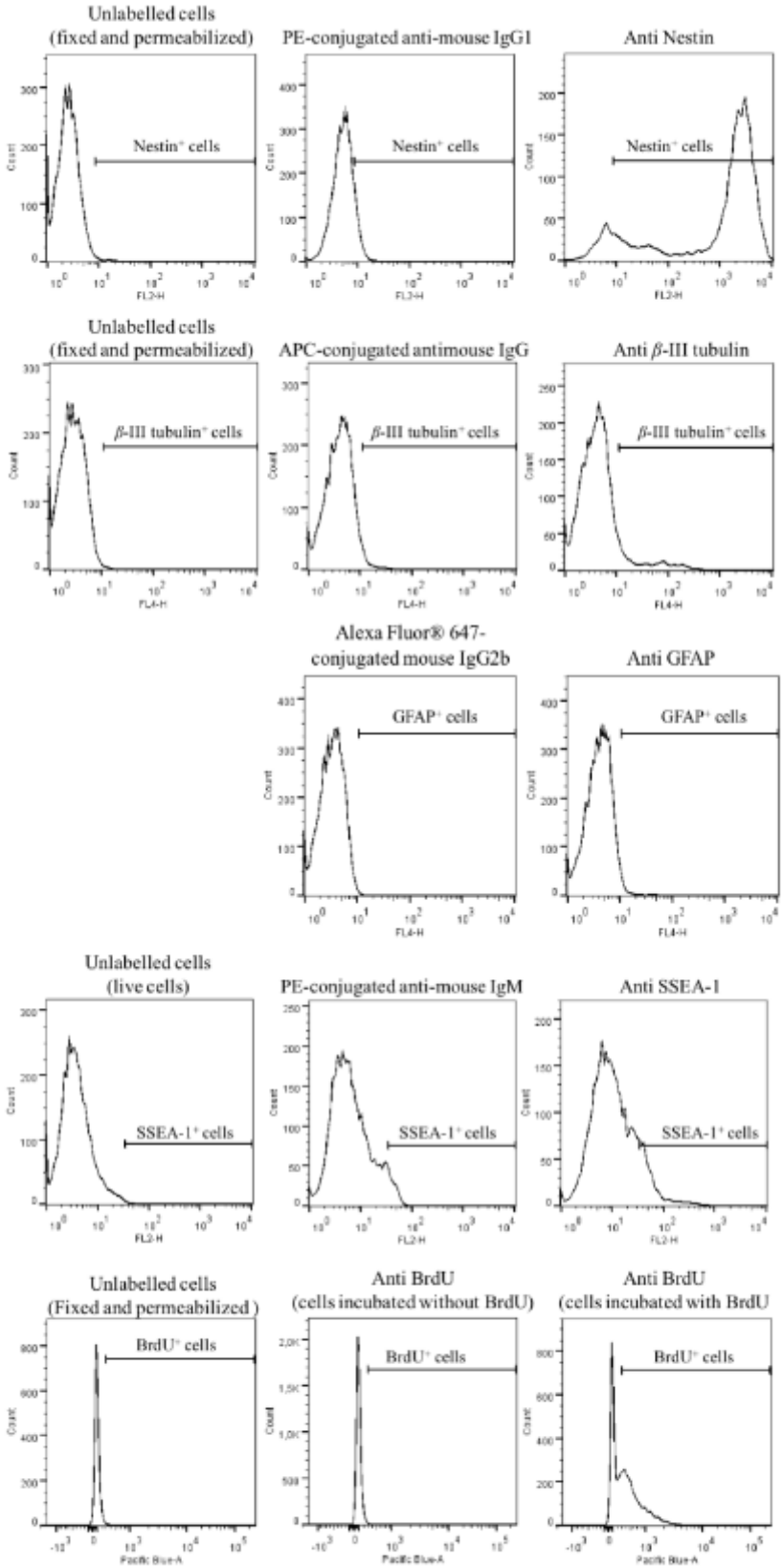

Figure S4 – Representative flow cytometry histograms obtained for the phenotypic and proliferation analysis of ES-NSPC neurospheres formed under static conditions. Cell debris and doublets were excluded by gating on forward and side scatter and fluorescence gates set using unlabeled cells processed in parallel. Cells stained with secondary antibody only or with the correspondent isotype control (Alexa Fluor® 647 Mouse IgG2b) were used to eliminate nonspecific background secondary antibody staining. In BrdU analysis, samples not exposed to BrdU but processed in parallel for immunodetection of BrdU were used as negative control.

A01/00

INSTITUTO
DE INVESTIGAÇÃO
E INOVAÇÃO
EM SAÚDE
UNIVERSIDADE
DO PORTO

Rua Alfredo Allen, 208
4200-135 Porto
Portugal
+351 220 408 800
info@i3s.up.pt
www.i3s.up.pt

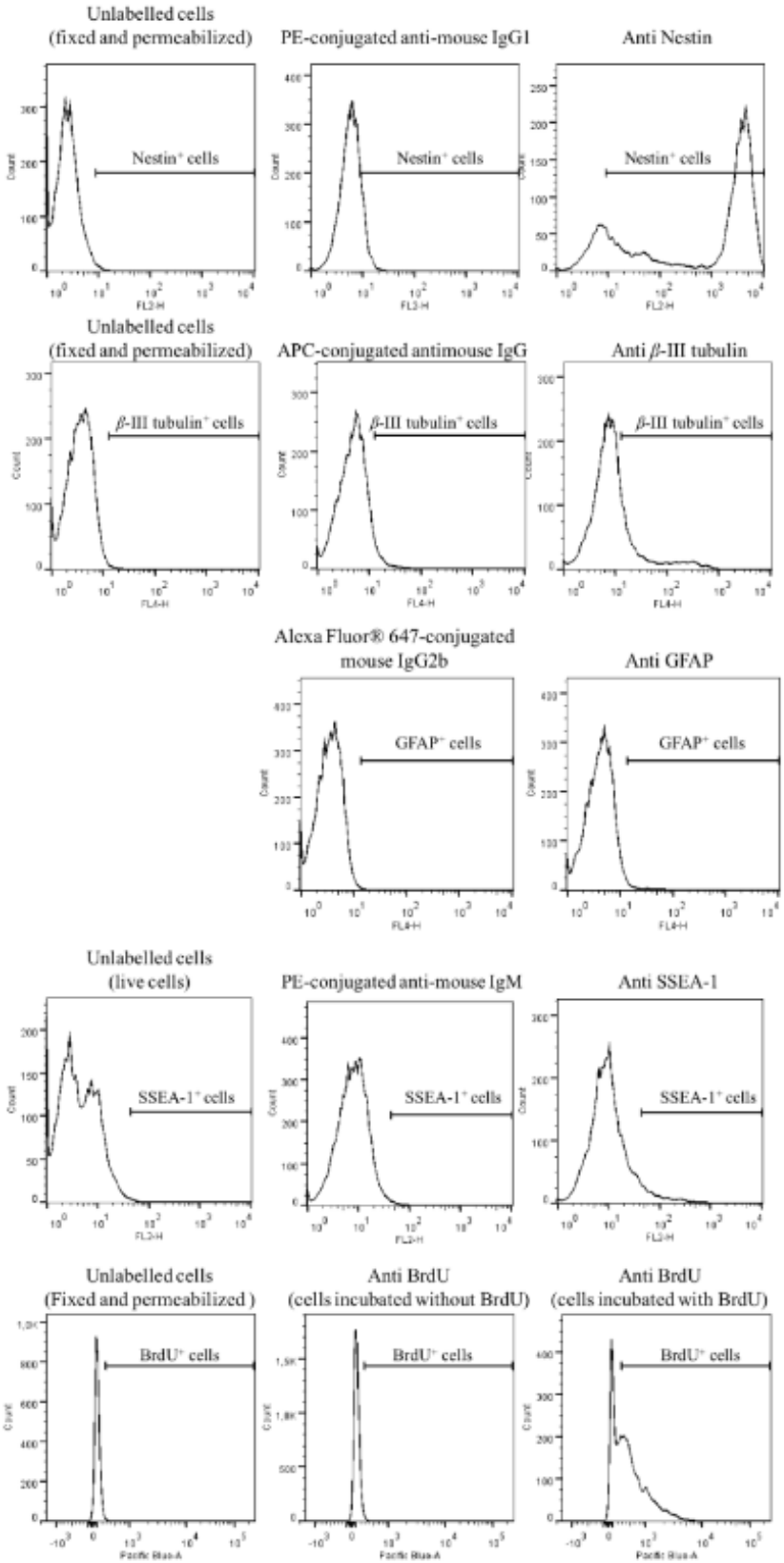

Figure S5 – Representative flow cytometry histograms obtained for the phenotypic and proliferation analysis of ES-NSPC neurospheres formed under hydrodynamic (55 rpm) conditions. Cell debris and doublets were excluded by gating on forward and side scatter and fluorescence gates set using unlabeled cells processed in parallel. Cells stained with secondary antibody only or with the correspondent isotype control (Alexa Fluor® 647 Mouse IgG2b) were used to eliminate nonspecific background secondary antibody staining. In BrdU analysis, samples not exposed to BrdU but processed in parallel for immunodetection of BrdU were used as negative control.

A01/00

INSTITUTO
DE INVESTIGAÇÃO
E INOVAÇÃO
EM SAÚDE
UNIVERSIDADE
DO PORTO

Rua Alfredo Allen, 208
4200-135 Porto
Portugal
+351 220 408 800
info@i3s.up.pt
www.i3s.up.pt

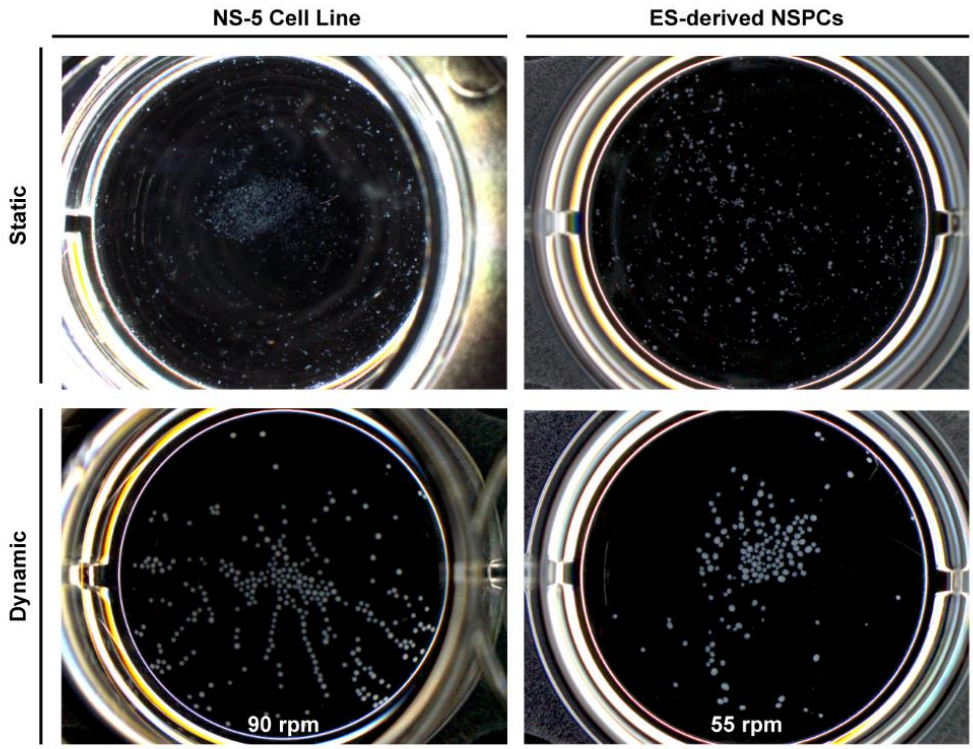

Figure S6 – Population of cellular aggregates of NS-5 cells and ES-NSPCs (neurospheres) formed under static and hydrodynamic conditions (90 or 55 rpm), after 72 h of cell culture. Neurospheres were transferred to the wells of a 24-well plate and dark field images of the wells acquired using an optical stereoscopic magnifier for latter image analysis and yield assessment. Rotary orbital suspension culture allowed the formation of homogeneously-sized neurospheres in both NS-5 and ES-NSPC suspension cultures.

INSTITUTO
DE INVESTIGAÇÃO
E INOVAÇÃO
EM SAÚDE
UNIVERSIDADE
DO PORTO

Rua Alfredo Allen, 208
4200-135 Porto
Portugal
+351 220 408 800
info@i3s.up.pt
www.i3s.up.pt

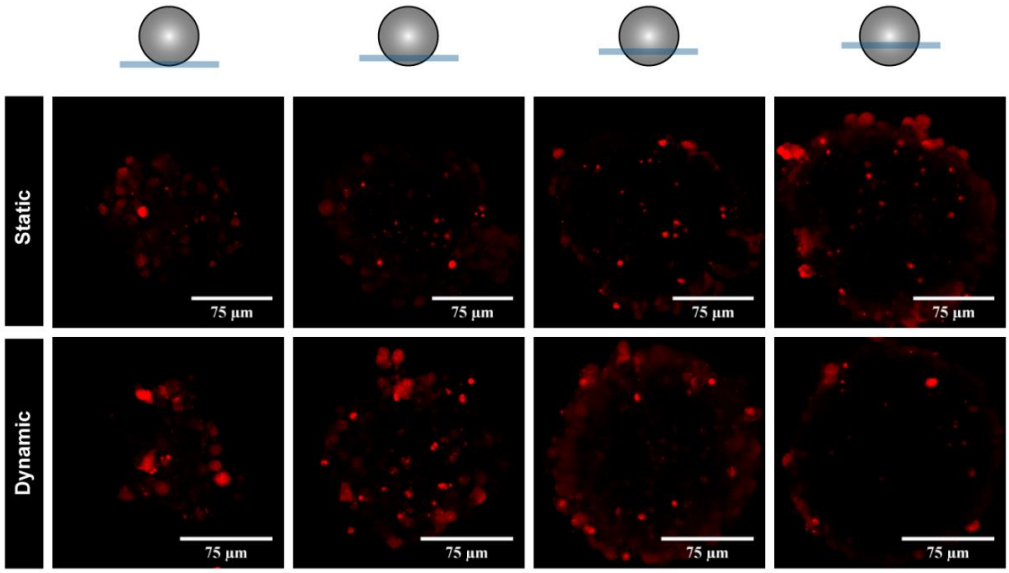

Figure S7 – Distribution of non-viable cells in ES-NSPC neurospheres formed under hydrodynamic (55 rpm) or static conditions. ES-NSPCs were cultured under suspension conditions for 72 h, incubated with propidium iodide, and imaged by CLSM. Images show 2-D projections of CLSM 3-D stack images covering each a depth of 21 µm, from the surface to the core of the neurosphere (total depth analyzed: 85 µm). In both types of neurospheres non-viable cells were found evenly distributed and necrotic cores were not observed.

INSTITUTO
DE INVESTIGAÇÃO
E INOVAÇÃO
EM SAÚDE
UNIVERSIDADE
DO PORTO

Rua Alfredo Allen, 208
4200-135 Porto
Portugal
+351 220 408 800
info@i3s.up.pt
www.i3s.up.pt

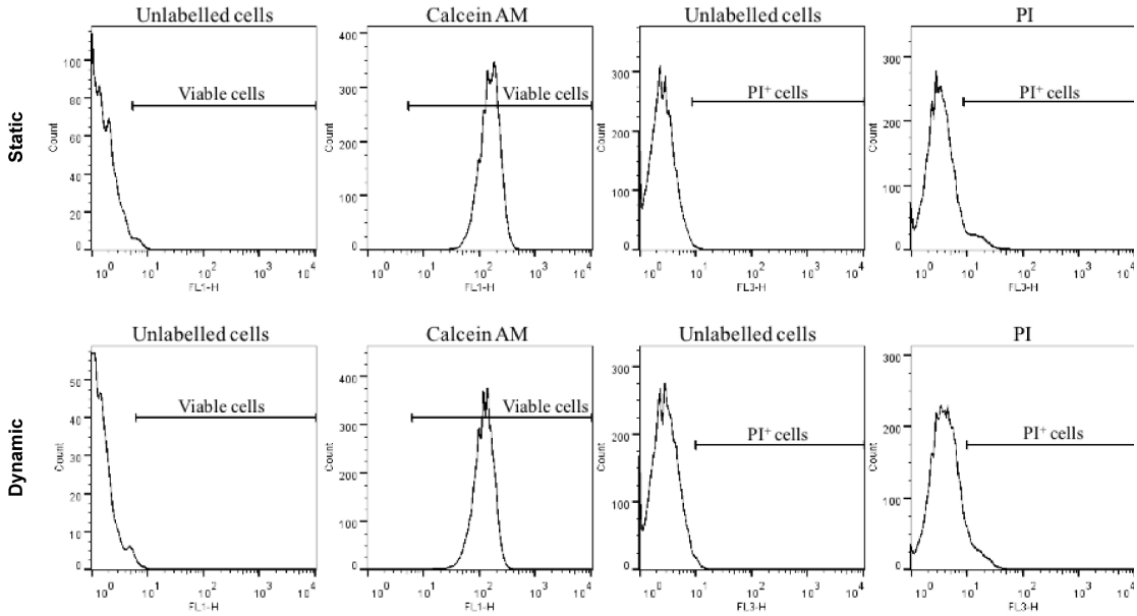

Figure S8 – Representative fluorescence flow cytometry histograms obtained for cell viability analysis of ES-NSPC neurospheres formed under static or hydrodynamic (55 rpm) conditions. ES-NSPC neurospheres were dissociated with StemPro® Accutase®, incubated with calcein AM (for detection of viable cells) or PI (for detection of dead cells), and analyzed by flow cytometry. Cell debris and doublets were excluded by gating on forward and side scatter and fluorescence gates set using unlabeled cells (negative control).

Calcein AM freely diffuses into the cells, being hydrolyzed by nonspecific esterases into bright green fluorescent products that are retained by cells. Propidium iodide (PI) enters cells with compromised membranes where it binds to nucleic acids producing intense red fluorescence.

INSTITUTO
DE INVESTIGAÇÃO
E INOVAÇÃO
EM SAÚDE
UNIVERSIDADE
DO PORTO

Rua Alfredo Allen, 208
4200-135 Porto
Portugal
+351 220 408 800
info@i3s.up.pt
www.i3s.up.pt

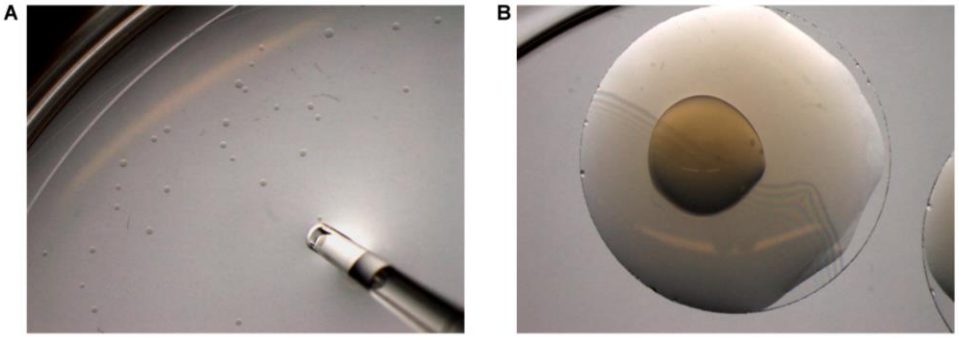

Figure S9 – Neurospheres embedding within fibrin hydrogels. (A) Isolation of neurospheres of 200 to 250 µm in diameter, under the stereoscopic magnifier. (B) Top view of the 3-D fibrin culture system used. A 50 µL fibrin drop was initially formed on the bottom of the Petri dishes (6 fibrin drops per Petri dish). Neurospheres (3 per fibrin drop) were subsequently embedded in a 20 µL drop of fibrin polymerizing solution formed on the top of the first fibrin drop. The presence of an under layer of fibrin assures the maintenance of a 3-D environment throughout the cell culture period.

INSTITUTO
DE INVESTIGAÇÃO
E INOVAÇÃO
EM SAÚDE
UNIVERSIDADE
DO PORTO

Rua Alfredo Allen, 208
4200-135 Porto
Portugal
+351 220 408 800
info@i3s.up.pt
www.i3s.up.pt

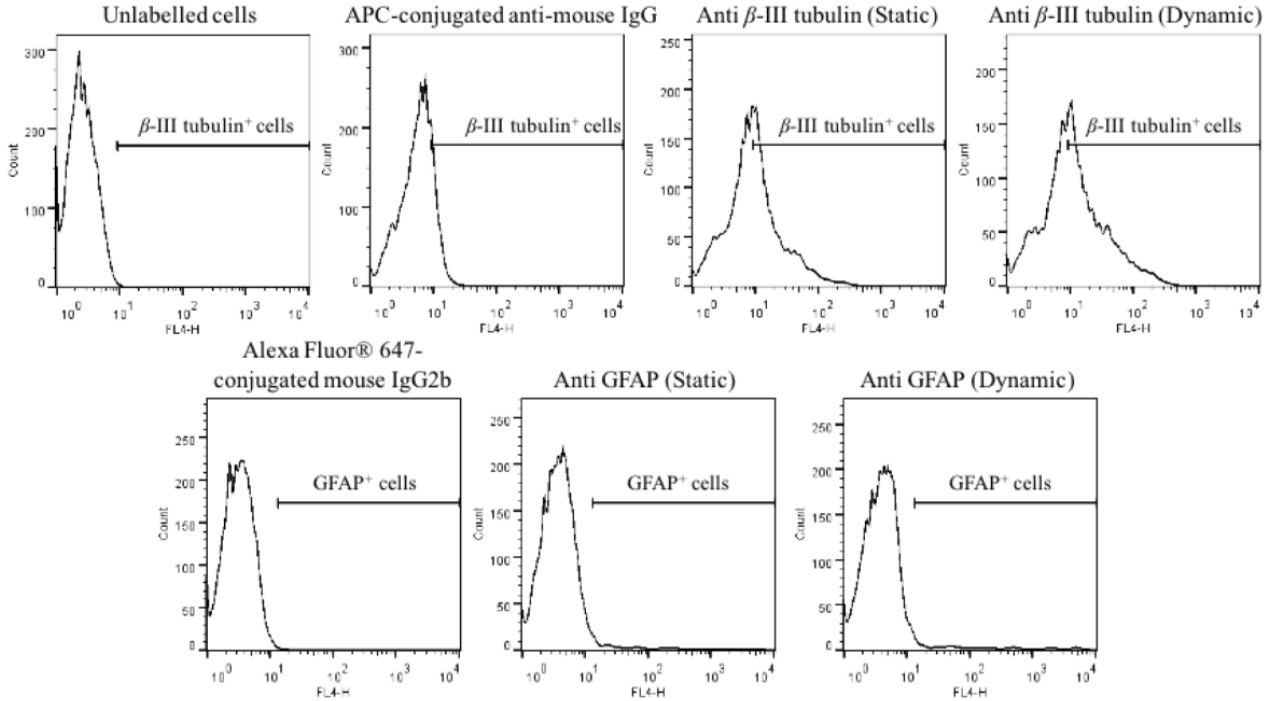

Figure S10 – Representative flow cytometry histograms obtained for the phenotypic analysis of ES-NSPC neurospheres cultured in fibrin. Neurospheres formed under static or hydrodynamic (55 rpm) conditions were embedded in fibrin hydrogels and cultured for 14 days under neuronal differentiation conditions. At day 14 of cell culture cells were isolated from the fibrin matrices and processed for flow cytometry analysis. Cell debris were excluded by gating on forward and side scatter and unlabeled cells (fixed and permeabilized) processed in parallel used to set fluorescence gates. For β-III tubulin staining, cells labelled with secondary antibody only (APC-conjugated goat anti-mouse IgG) were used as negative control. For GFAP staining, cells were incubated with an Alexa Fluor® 647 conjugated primary antibody, and Alexa Fluor® 647 Mouse IgG2b used as negative control.

INSTITUTO DE INVESTIGAÇÃO E INOVAÇÃO EM SAÚDE
UNIVERSIDADE DO PORTO

Rua Alfredo Allen, 208
4200-135 Porto
Portugal
+351 220 408 800
info@i3s.up.pt
www.i3s.up.pt

S9

A

NS-5 Cell Line

Size

	60 rpm	70 rpm	80 rpm	90 rpm	110 rpm	130 rpm	150 rpm
Static	**	***	**	***	***	**	*
60 rpm		**	**	***	***	***	***
70 rpm			**	***	***	***	***
80 rpm				ns	*	**	***
90 rpm					*	**	***
110 rpm						*	***
130 rpm							**

Yield

	60 rpm	70 rpm	80 rpm	90 rpm	110 rpm	130 rpm	150 rpm
Static	*	*	*	*	**	*	**
60 rpm		*	***	***	*	***	**
70 rpm			*	***	**	**	**
80 rpm				***	*	**	*
90 rpm					ns	*	*
110 rpm						ns	*
130 rpm							*

B

ES-derived NSPCs

Size

	50 rpm	55 rpm	60 rpm	70 rpm
Static	***	*	ns	ns
50 rpm		ns	**	***
55 rpm			*	*
60 rpm				ns

Yield

	50 rpm	55 rpm	60 rpm	70 rpm
Static	*	*	*	*
50 rpm		**	***	***
55 rpm			**	**
60 rpm				**

INSTITUTO DE INVESTIGAÇÃO E INOVAÇÃO EM SAÚDE
UNIVERSIDADE DO PORTO

Rua Alfredo Allen, 208
4200-135 Porto
Portugal
+351 220 408 800
info@i3s.up.pt
www.i3s.up.pt

Table S2 – Solutions and primary antibodies used in immunocytochemistry.

Marker	Permeabilization/ DNA denaturation	Blocking buffer	Primary antibody			
			Name	Ref.	Company	Dilution
BrdU	1) 0.2% (v/v) Triton X-100 in PBS (10 min) 2) 2M HCl (20 min)	5% (v/v) NGS in PBS containing 0.05% (v/v) Tween-20	Mouse Anti-bromodeoxyuridine, (clone Bu20a)	M074	DAKO	1:10
β-catenin	1) 50 mM NH_4Cl in PBS (10 min) 2) 0.2% (v/v) Triton X-100 in PBS (5 min)	5% (v/v) BSA in PBS	Mouse Anti β-Catenin	610154	BD Transduction Labs	1:100
N-cadherin	None	10% FBS (v/v) in PBS containing 0.05% (v/v) Tween-20	Mouse Anti N-Cadherin	610920	BD Transduction Labs	1:200
Laminin		1% (v/v) BSA and 4% (v/v) FBS in PBS	Rabbit anti-laminin	L9393	Sigma	1:50
Fibronectin		5% (v/v) BSA in PBS	Rabbit anti-fibronectin	F3648	Sigma;	1:100
SSEA-1		5% (v/v) NGS in PBS	Mouse stage specific embryonic antigen 1 marker (clone 480)	sc-21702	Santa Cruz Biotech.	1:100
Nestin	0.2% (v/v) Triton X-100 in PBS (10 min)	5% (v/v) NGS in PBS containing 0.05% (v/v) Tween-20	Mouse Anti nestin antibody (clone rat-401)	MAB353	Chemicon	1:100
β-III tubulin		5% (v/v) horse serum and 3% (v/v) BSA in PBS containing 0.05% (v/v) Tween-20	Rabbit Anti β III tubulin antibody	ab18207	Abcam	1:500
GFAP			Rabbit Anti-Glial Fibrillary Acidic Protein	Z 0334	DAKO	1:500

Abbreviations: BrdU, 5-Bromo-2'-deoxyuridine; NGS, normal goat serum; BSA, bovine serum albumin; FBS, fetal bovine sérum; SSEA-1, stage-specific embryonic antigen 1; GFAP, glial fibrillary acidic protein.

INSTITUTO DE INVESTIGAÇÃO E INOVAÇÃO EM SAÚDE
UNIVERSIDADE DO PORTO

Rua Alfredo Allen, 208
4200-135 Porto
Portugal
+351 220 408 800
info@i3s.up.pt
www.i3s.up.pt

Table S3 – Solutions and primary antibodies used in immunocytometry.

Marker	Permeabilization/ DNA denaturation	Blocking buffer	Primary antibody/isotype control			
			Name	Ref.	Company	Dilution
BrdU	1) 1% (w/v) PFA (20 min) 2) 0.2% (v/v) Triton X-100 in PBS (10 min) 3) 2M HCl (20 min)	5% (v/v) NGS in PBS containing 0.1% (w/v) Saponin	V450-conjugated anti-BrdU	560810	BD Horizon	8 µg/mL
Nestin	1) 1% (w/v) PFA (20 min) 2) 0.2% (v/v) Triton X-100 in PBS (10 min)		Mouse Anti nestin (clone rat-401)	MAB353	Chemicon	1:100
β-III tubulin			Mouse Anti β III tubulin	MMS-435P	Covance	1:500
GFAP			Alexa Fluor 647 mouse anti-GFAP	561470	BD Pharmigen	1:100
			Alexa Fluor® 647 Mouse IgG2b isotype control	558713	BD Pharmigen	1:100
SSEA-1	None	5% (v/v) NGS in PBS	Mouse stage specific embryonic antigen 1 marker (clone 480)	sc-21702	Santa Cruz Biotech.	1:100

Abbreviations: BrdU, 5-Bromo-2'-deoxyuridine; PFA, paraformaldehyde; NGS, normal goat serum; GFAP, glial fibrillary acidic protein; SSEA-1, stage-specific embryonic antigen.

INSTITUTO DE INVESTIGAÇÃO E INOVAÇÃO EM SAÚDE
UNIVERSIDADE DO PORTO

Rua Alfredo Allen, 208
4200-135 Porto
Portugal
+351 220 408 800
info@i3s.up.pt
www.i3s.up.pt